

# Simulation studies of a micro bulk XY-Micromegas detector for neutron-induced charged particle tracking

G. Tsiledakis  
CEA Irfu, University Paris-Saclay  
France  
[georgios.tsiledakis@cea.fr](mailto:georgios.tsiledakis@cea.fr)

E. Berthoumieux, E. Dupont, F. Gunsing

# Contents

- Micromegas concept
- XY-micromegas detector
- Experimental results in Orphee reactor using a XY-micromegas as neutron beam profiler
- Neutron reactions for thermal neutron detection: SRIM / SDtrimSP codes
- Basic set-up approximation used in simulations
- Using FLUKA MC code
- New XY-micromegas detector  $10 \times 10 \text{ cm}^2$
- Garfield++ → methods, magnitude of diffusion, induced charge, convoluted pulses...
- FLUKA energy deposition spectrum vs Garfield++ deposited charge
- Summary
- Outlook

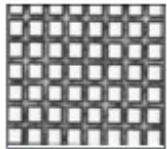
# Neutron detectors based on MICRO-Mesh Gaseous Structure (MICROMEAS)

## Micro-mesh (cathode)

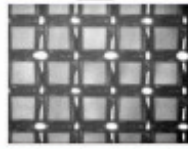
The metallic micro-mesh must be 5 to 30  $\mu\text{m}$  thick with needed equivalent wires densities ranging from 500 to 2000 Lines Per Inch (LPI). Stainless steel woven meshes, electroformed Nickel meshes, or chemically etched copper meshes are used.

New products are needed for high LPI thin meshes.

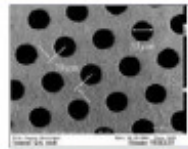
500 LPI Electroformed Ni mesh



500 LPI 304L woven mesh

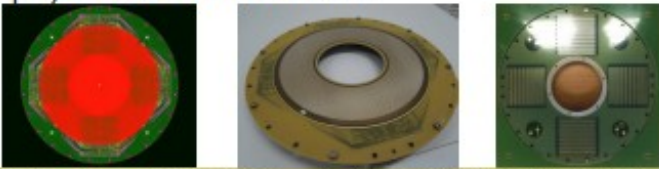


Chemically etched Copper mesh



## Printed Circuit Board (anode PCB)

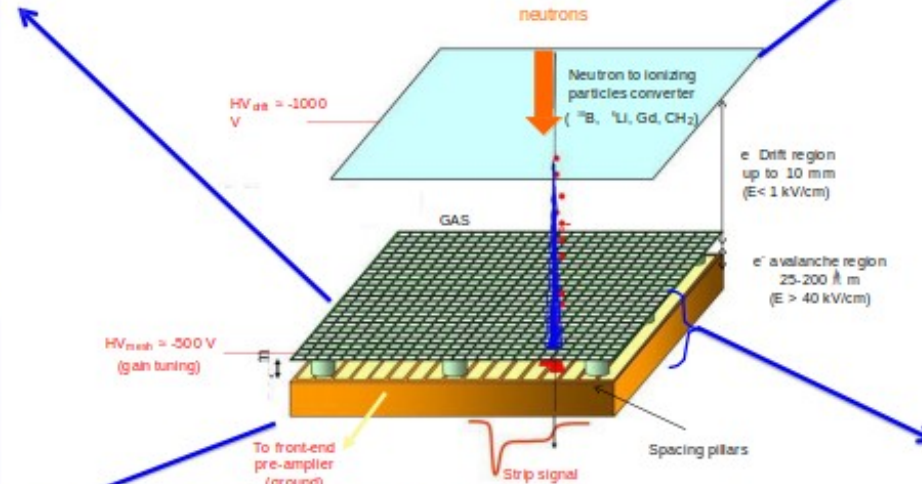
- ✓ It can be up to 1- 3  $\text{m}^2$  and down to 100  $\mu\text{m}$  thin.
- ✓ Copper strips or pads can be  $\approx 100 \mu\text{m}$  to few mm large and insulation between them as low as 50  $\mu\text{m}$ .
- ✓ Copper is usually covered by a Ni/Au layer for a total thickness which must be kept as low as possible (down to 5  $\mu\text{m}$ ) with a « smooth » surface.



A  $\phi$  30 cm 12 layers PCB with 4000 x 4 mm pads for the MINOS TPC (18000 blind vias)

Patented technology (CEA – EOS imaging)  
G. Charpak, Y. Giomataris, Ph. Rebourgeard, J-P Robert  
Y. Giomataris et al., NIMA 376 (1996) 29

MICROMEAS is a parallel plate gaseous structure which uses a thin metallic micro-mesh to define the high electric field region in which primary electrons are amplified by avalanche and collected on a micro-segmented Printed Circuit Board



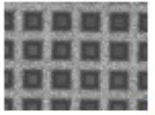
## Performances

- ✓ Intrinsic low sensitivity to  $\gamma$  photons (gas)
- ✓ High spatial resolution (down to 100  $\mu\text{m}$ )
- ✓ Fast signals (< 1 ns)
- ✓ Short recovery time ( $\sim 150$  ns)
- ✓ High rate capabilities (> MHz)
- ✓ High gain (up to  $10^6$ )

## Drift electrode + neutron converter

- ✓ For thermal neutrons, it can be a thin aluminum foil or a metallic mesh covered by a 1-2  $\mu\text{m}$  thick layer containing  $^{10}\text{B}$  (such as  $\text{B}_4\text{C}$ ) or by a  $\approx 100 \mu\text{m}$  thick  $^6\text{Li}$  layer. Low cost industrialized processes needed

An electroformed Ni mesh covered by a 2  $\mu\text{m}$  thick  $\text{B}_4\text{C}$  layer (L. Inkinging Univ.)



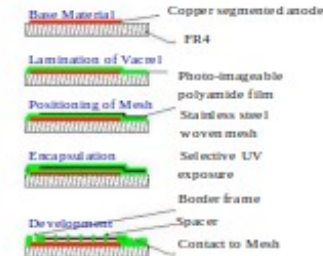
## Micromegas technologies

to realize the micro-mesh + anode PCB assembly

### Bulk-micromegas

On-going technology transfer

Embedding of the mesh between two layers of insulating pillars by use of photolithography technics

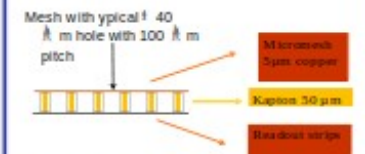


A Micromegas bulk assembly (D. NTFC)

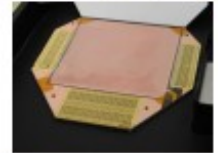
### micro-bulk micromegas

Technology transfer to be done

Micromegas is built from a double sided copper clad kapton foil by selective chemical etching of copper (mesh and anode strips) and kapton (insulating pillars).

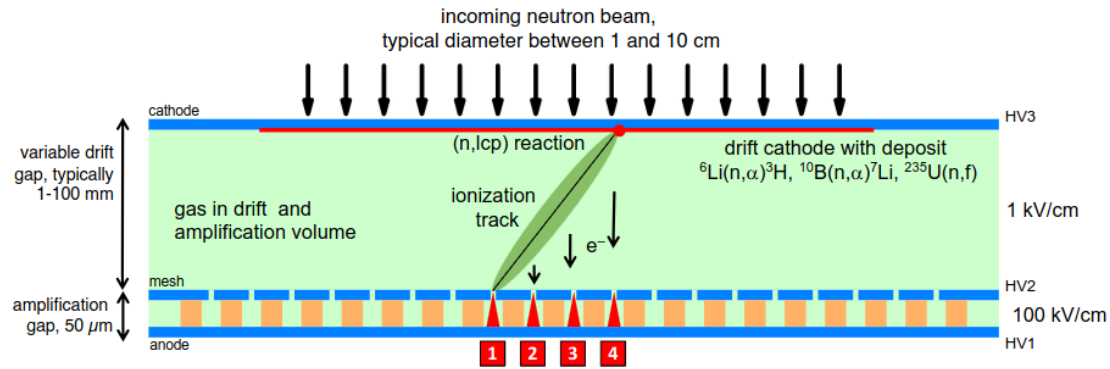


A 10x10  $\text{cm}^2$  micro-bulk (NEXT prototype)





# XY - micromegas detector



- 60 x 60 strips (6x6 cm<sup>2</sup>)
- Mesh hole ~ 60  $\mu\text{m}$
- Pitch: 100  $\mu\text{m}$

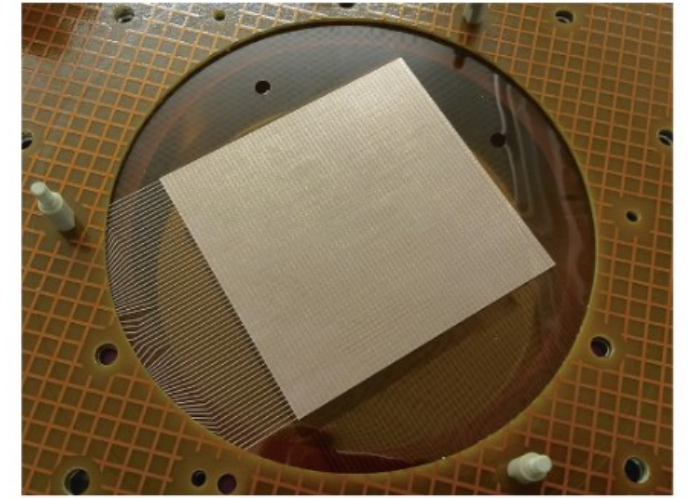


Fig. 2. (Colour online) Photo of the first 6 × 6 cm<sup>2</sup> segmented mesh microbulk detector produced, mounted on the thick PCB.

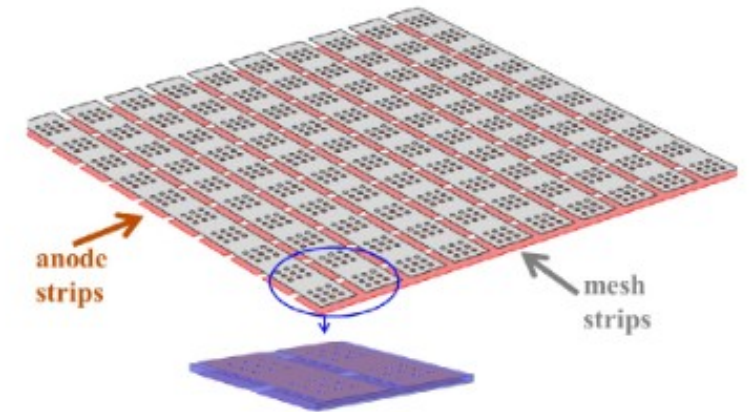
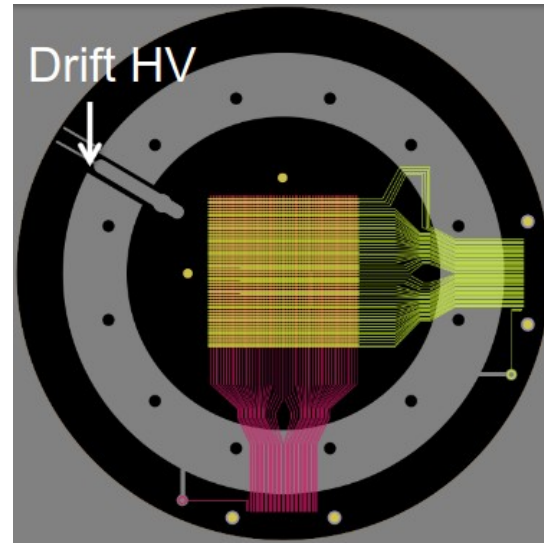
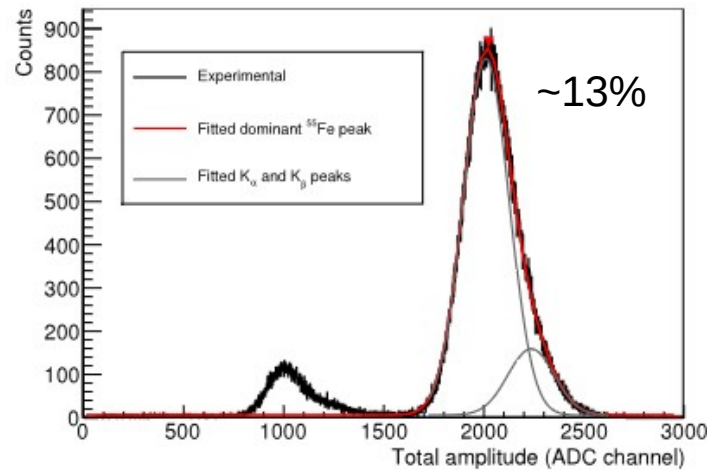
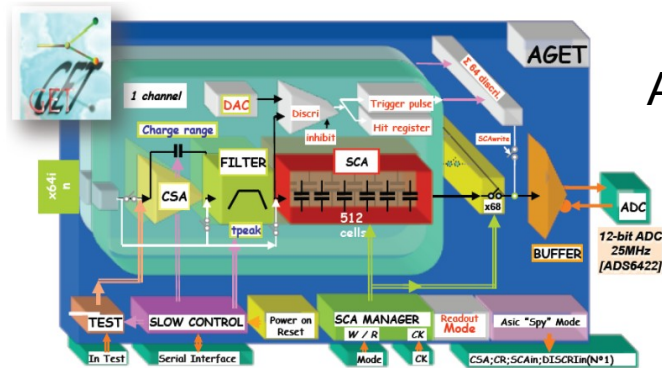
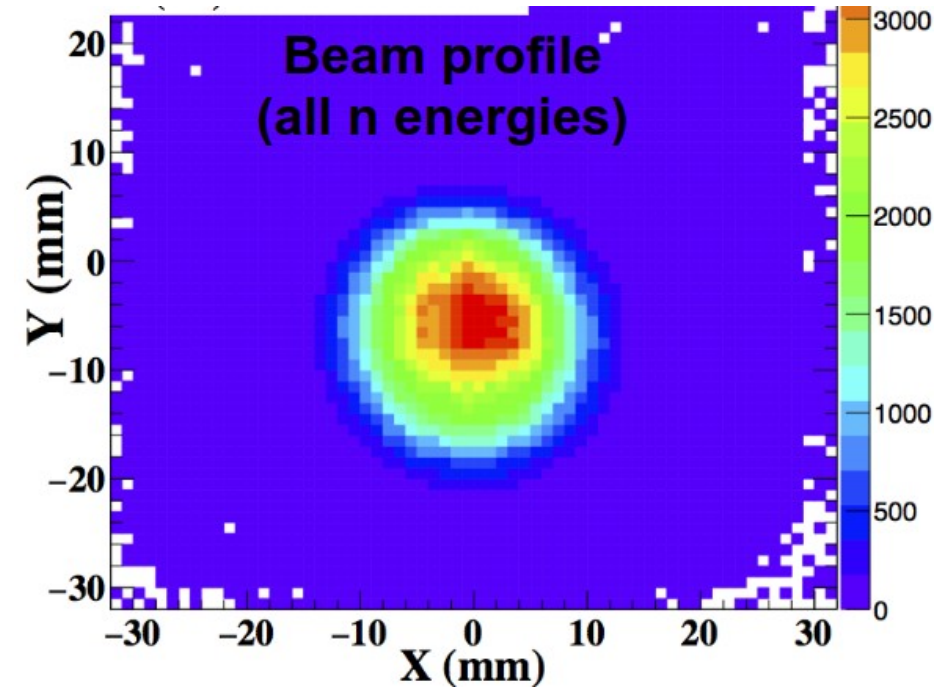
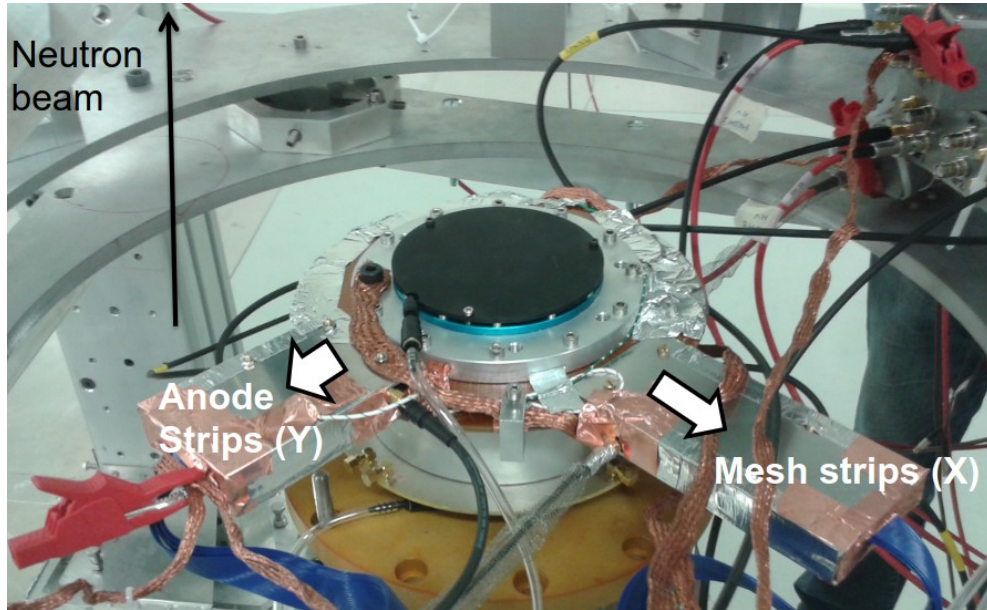


Fig. 1. (Colour online) Schematic view of the segmented mesh microbulk detector. The holes of the micromesh are arranged in matrices with a fixed number of holes/column in the overlapping region of mesh and anode strips.

Development of a novel segmented mesh MicroMegas detector for neutron beam profiling, <https://doi.org/10.1016/j.nima.2018.06.019>, Nuclear Inst. and Methods in Physics Research, A 903 (2018) 46–55

# XY - micromegas detector at CERN

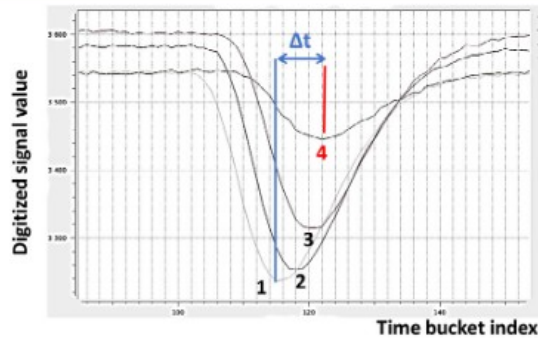
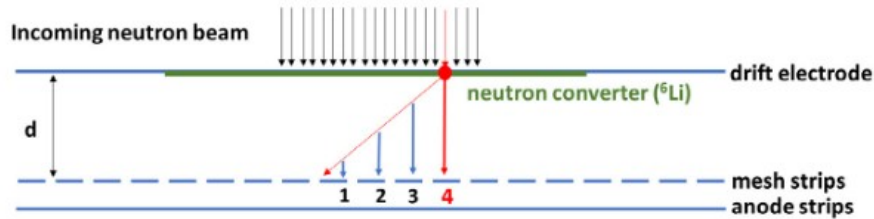


AGET electronics

Development of a novel segmented mesh MicroMegas detector for neutron beam profiling,  
<https://doi.org/10.1016/j.nima.2018.06.019>, Nuclear Inst. and Methods in Physics Research, A 903 (2018) 46–55



# Experimental results in Orphée reactor (LLB)



→ Simulate the experiment  
→ Reproduce the amplitude distribution histograms

→ Study the performance in the detection of the neutrons and the reconstruction of neutron beam profiles

→ Neutron kinetic energy of 3 meV

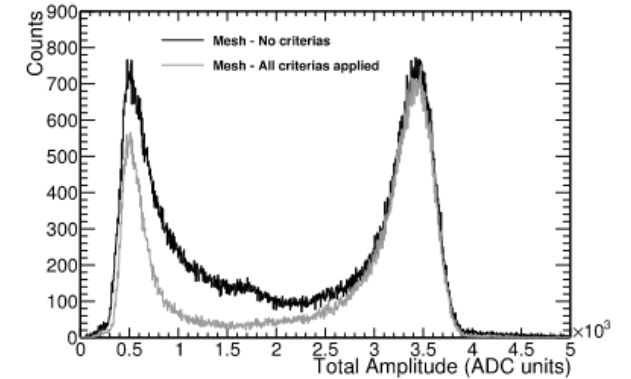
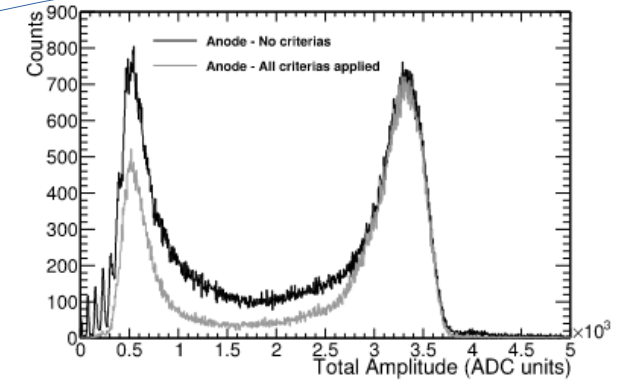
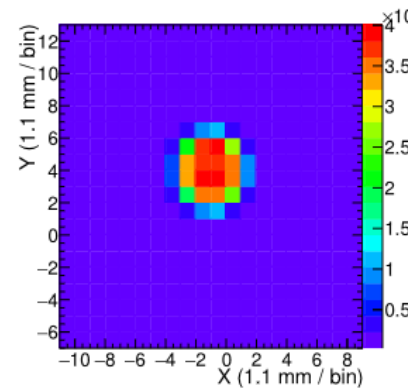


**Fig. 11.** Reconstructed total amplitude distribution histogram, by adding the amplitudes of all the strip signals in each event, for the anode (up) and the mesh (down), from all the events (black) and only from the selected ones with the criteria applied (grey).

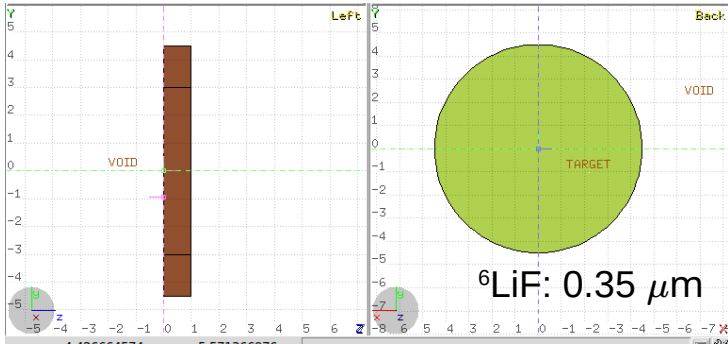
**Table 2**

Characteristics of the masks used. In most cases, PMMA plates were used in order to reduce the neutron fluence (by a factor of 16).

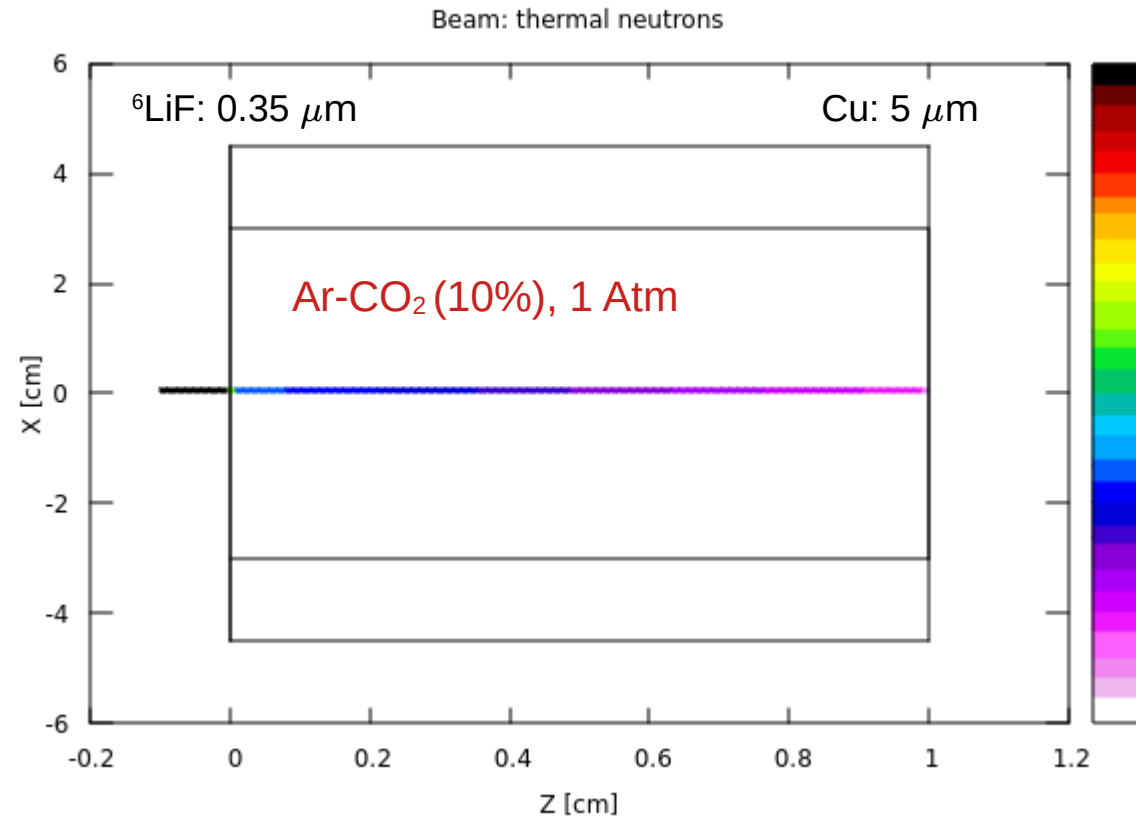
Mask shape	Dimensions (mm)
Circular hole	∅ 5
Circular hole	∅ 2
Square hole	5 × 5
Rectangular hole	1 × 5

Development of a novel segmented mesh MicroMegas detector for neutron beam profiling,  
<https://doi.org/10.1016/j.nima.2018.06.019>, Nuclear Inst. and Methods in Physics Research, A 903 (2018) 46–55

# Basic set-up: approximation - FLUKA simulations



Drift : 1 cm  
Size: 6 x 6 cm<sup>2</sup>



Frontiers in Physics 9, 788253 (2022).  
Annals of Nuclear Energy 82, 10-18 (2015).  
<https://fluka.cern>, <https://flair.cern/>

# ${}^6\text{LiF}$ target: Ion Penetration Distance – SRIM vs SDTrimSP

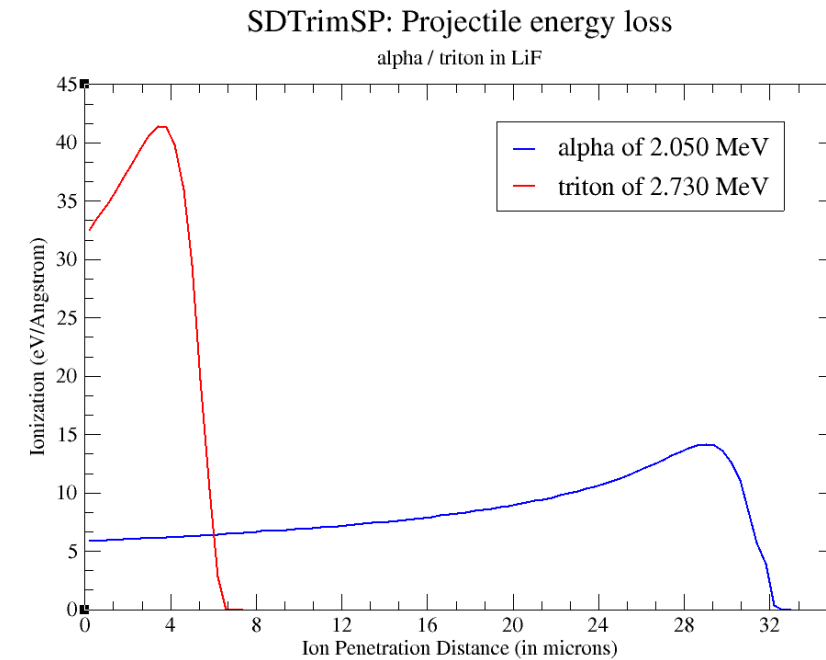
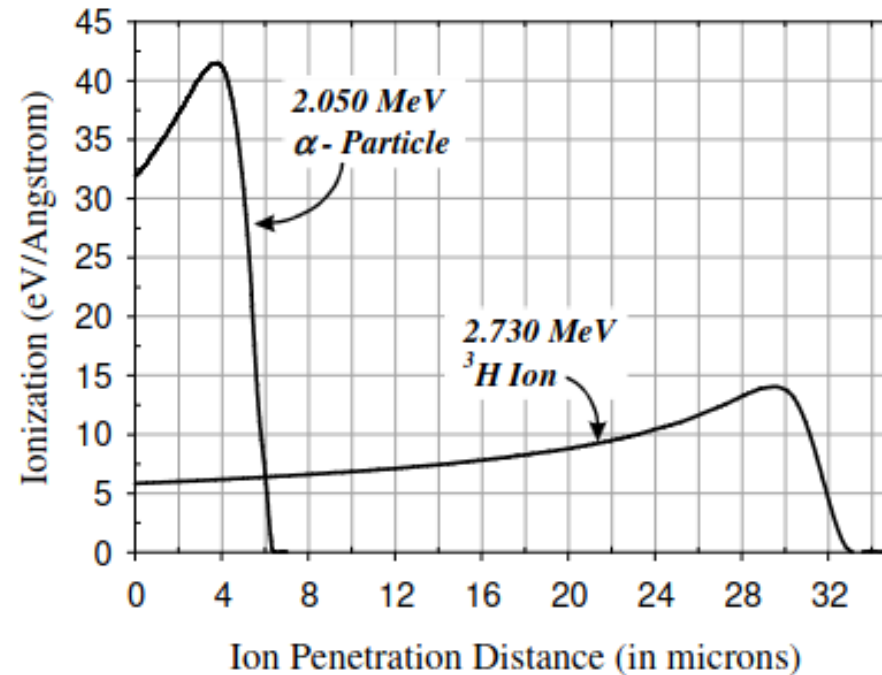
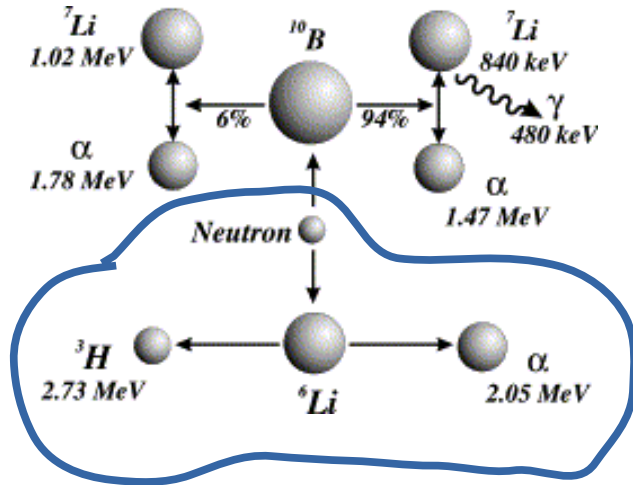


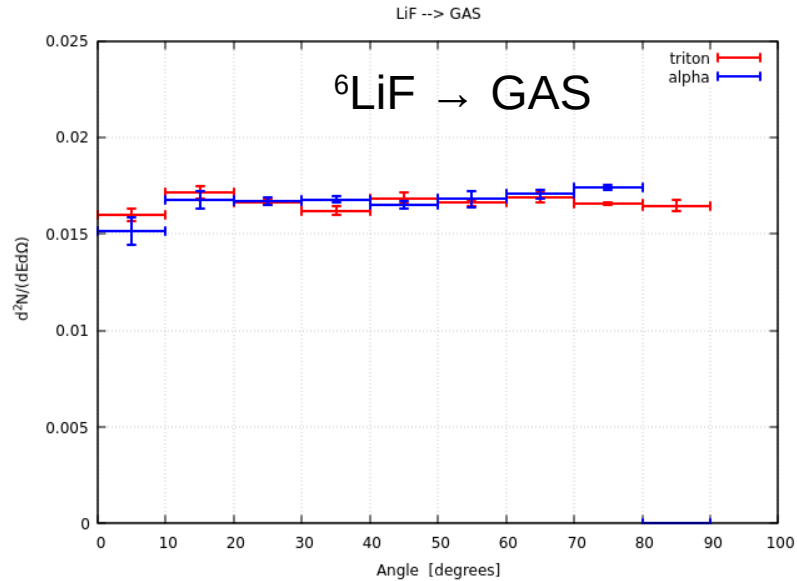
Fig. 7.  ${}^6\text{Li}(n, \alpha){}^3\text{H}$  reaction product energy loss in a  ${}^6\text{LiF}$  film as described by the Bragg distribution.

doi:10.1016/s0168-9002(02)02078-8

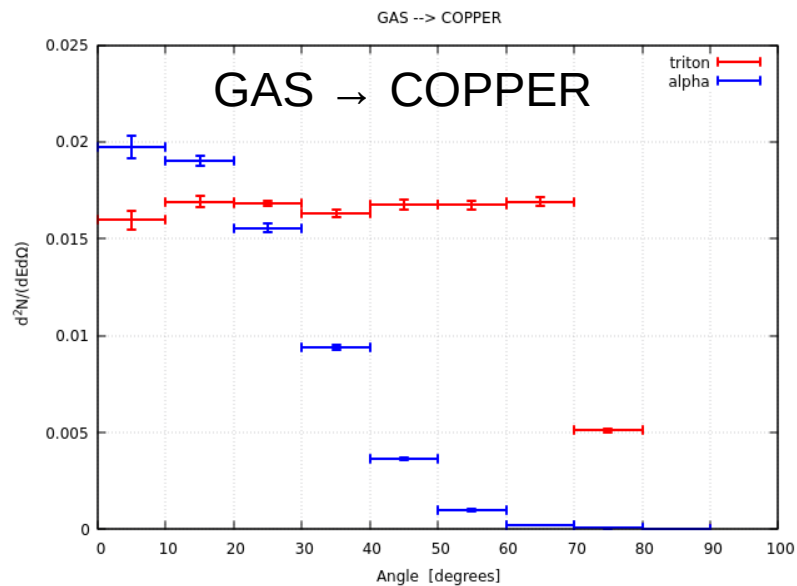
A. Mutzke et al.(2019), SDTrimSP Version 6.00 (IPP 2019-02). Garching: Max-Planck-Institut für Plasmaphysik. doi:10.17617/2.3026474.



# alpha / triton yield - FLUKA simulations

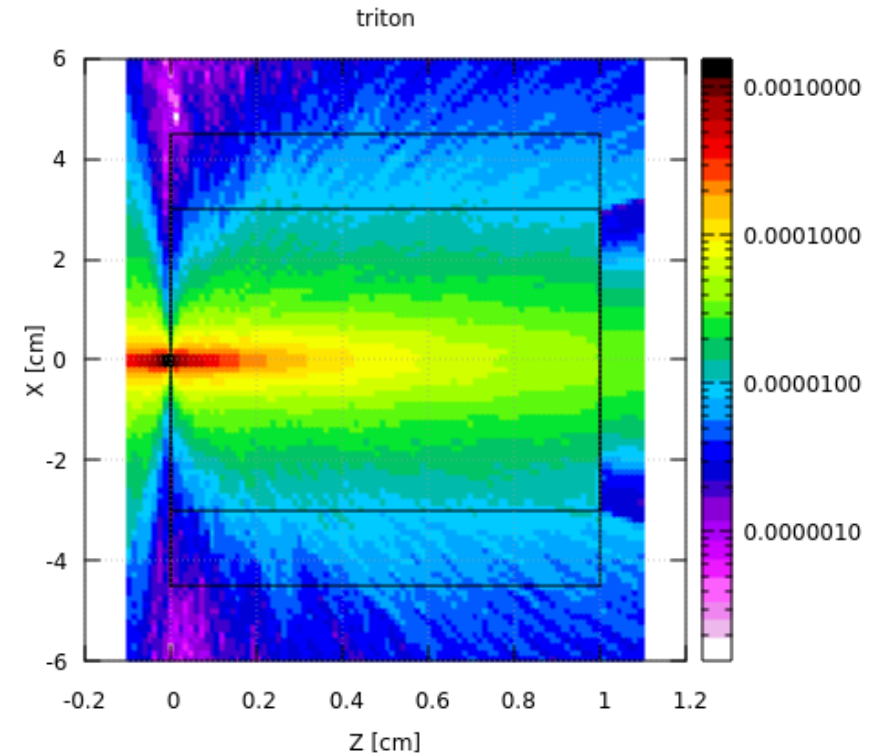
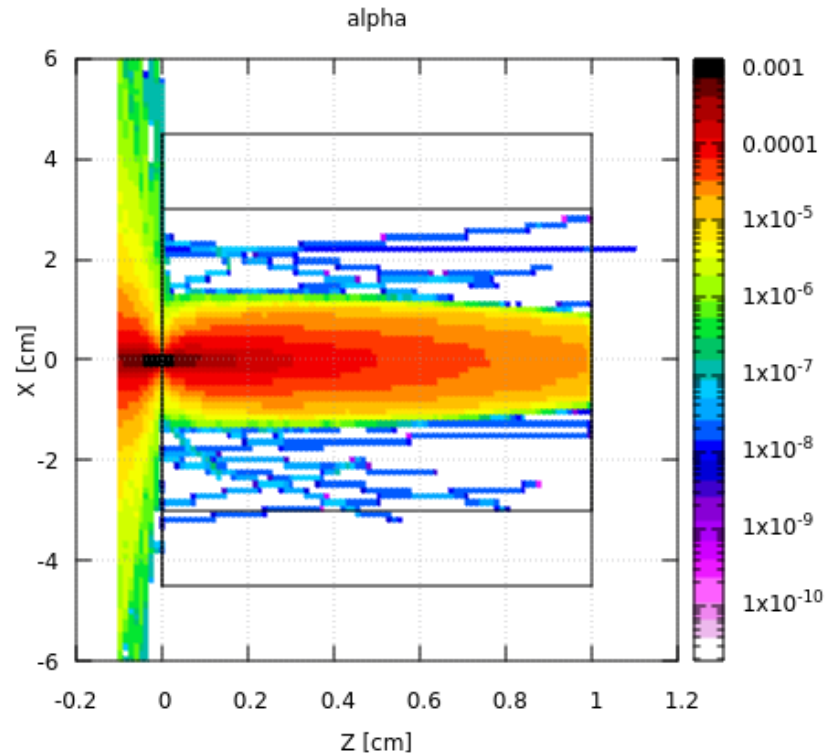


- Differential yield  $\rightarrow$  solid angle in steradian
- Angles with respect of the beam direction (polar angles in degrees) and results normalized as double differential, expressed in [particles  $\text{GeV}^{-1}\text{sr}^{-1}/\text{primary}$ ]



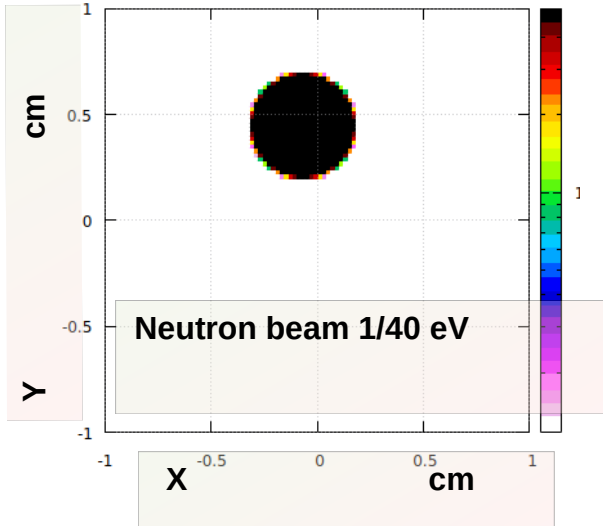
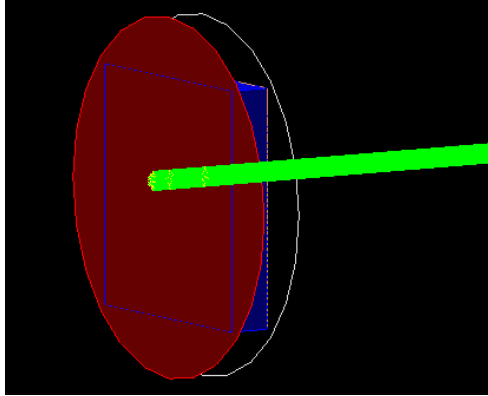
- $\rightarrow$  For a given neutron interaction point the direction the two capture fragments are emitted is isotropically distributed.
- $\rightarrow$  The detector response, depending on its geometry, will be different according to the particle ejection direction.
- $\rightarrow$  What is measured, when the detector is exposed to a point source, is an average over all the possibilities that results into a distribution with its own FWHM that defines the resolution due to the gas.

# alpha / triton fluence - FLUKA simulations

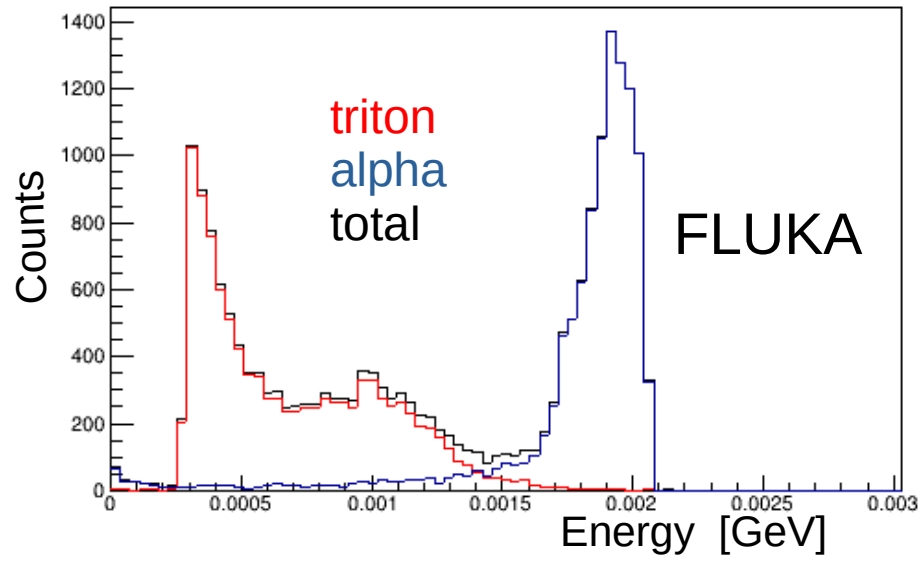
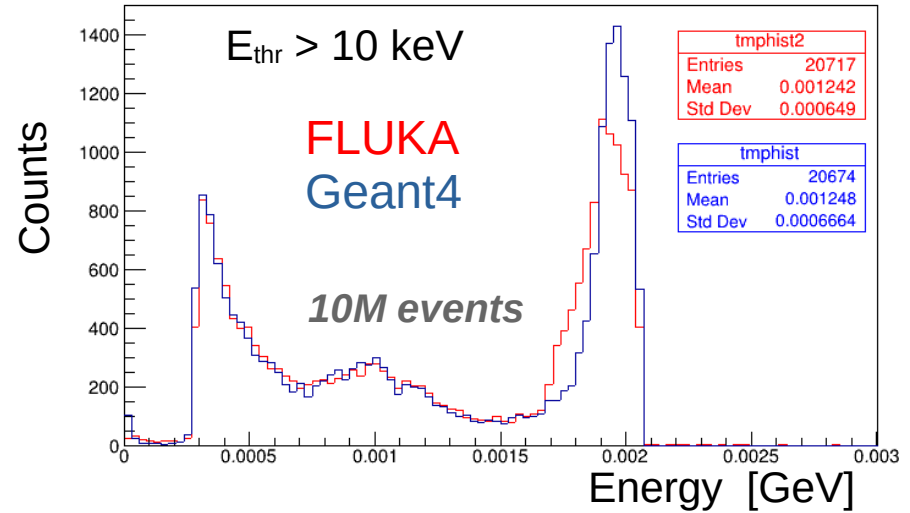


→ Track-length density in particles/cm<sup>2</sup> per primary

# FLUKA vs Geant4



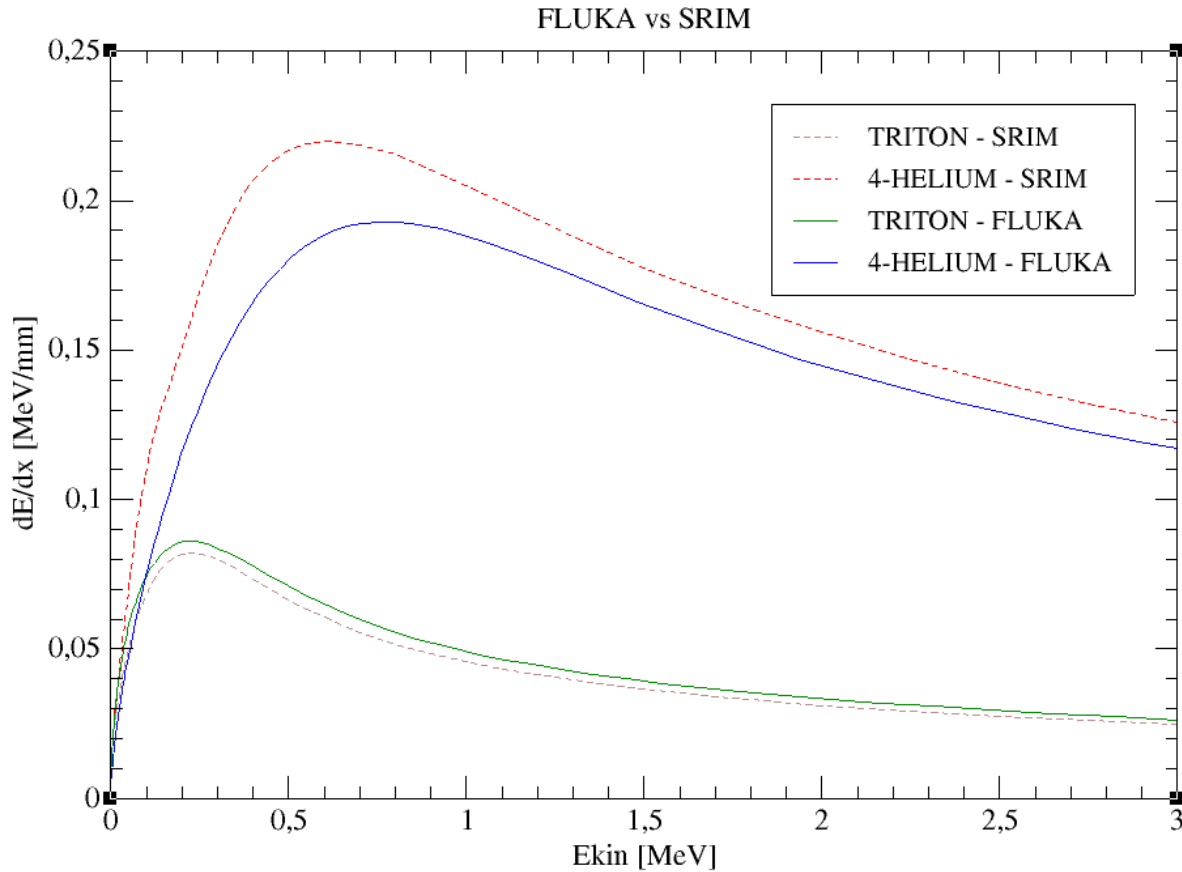
<https://geant4.web.cern.ch/>



Energy deposition spectra

# dE/dx: FLUKA vs SRIM

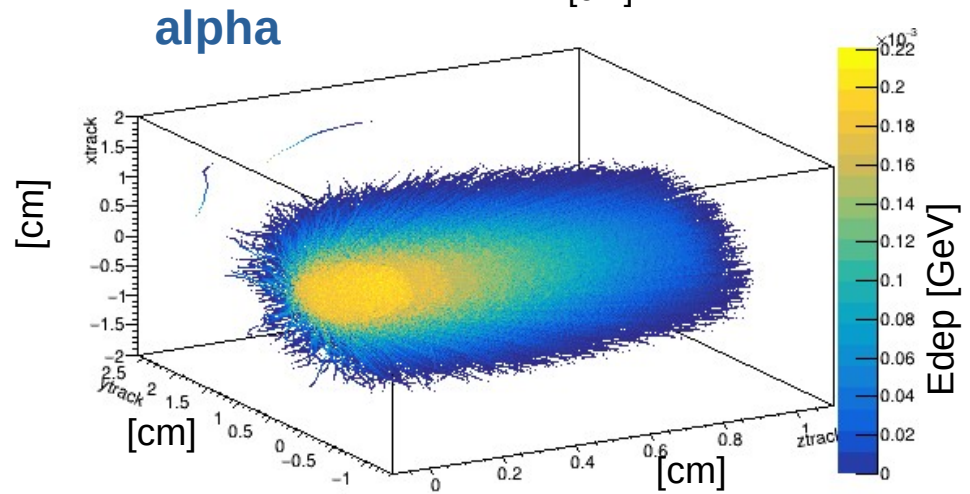
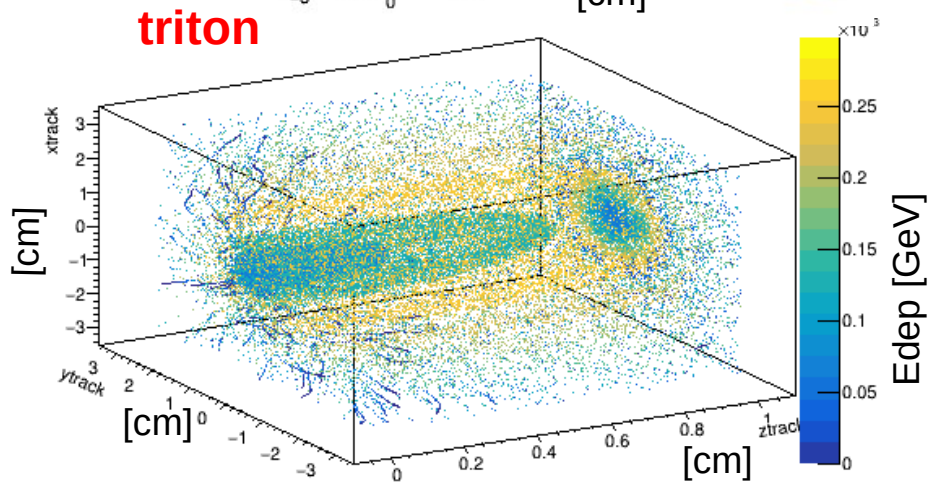
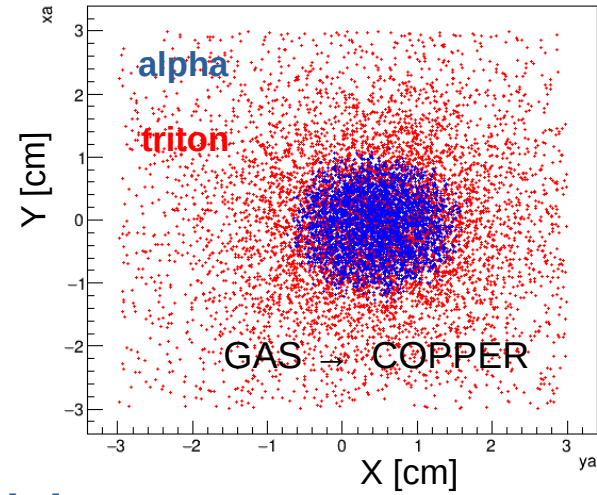
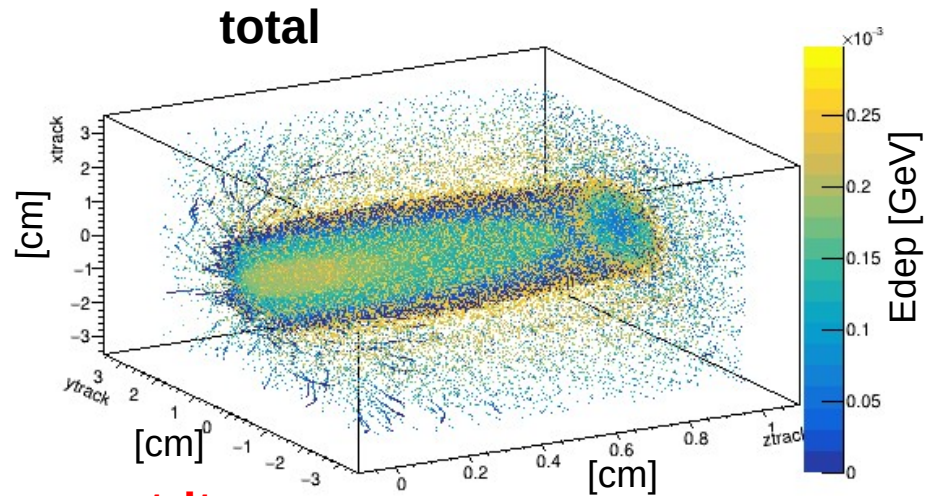
TRITON and 4-HELIUM Stopping Power in Ar-CO<sub>2</sub> (10%), 1 Atm



- Triton: FLUKA and SRIM are in perfect agreement
- Alpha: Underestimation in FLUKA ("different" stopping power recipe)

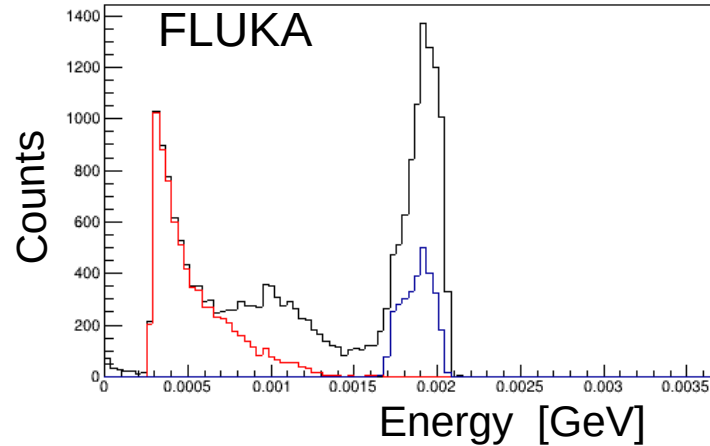


# MGDRAW: Energy deposition hits - FLUKA simulations

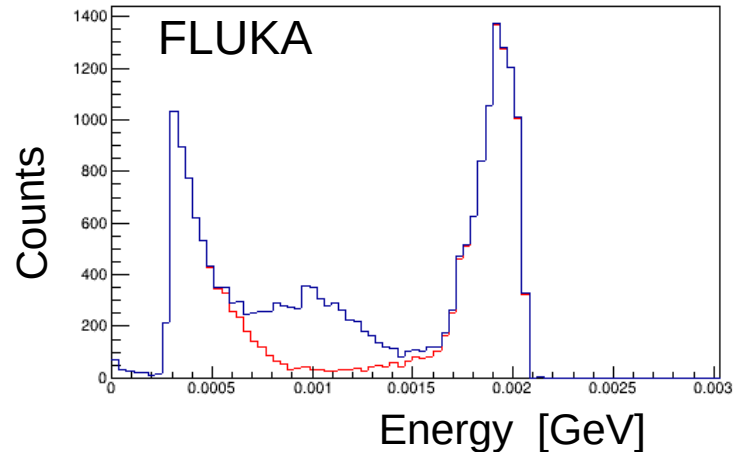


# Comparison with experimental data

No Cuts  
 triton:  $ztrack > 1 \text{ cm}$   
 alpha:  $ztrack > 1 \text{ cm}$



No Cuts  
 $|x,ytrack| < 2 \text{ cm}$



## Experimental data

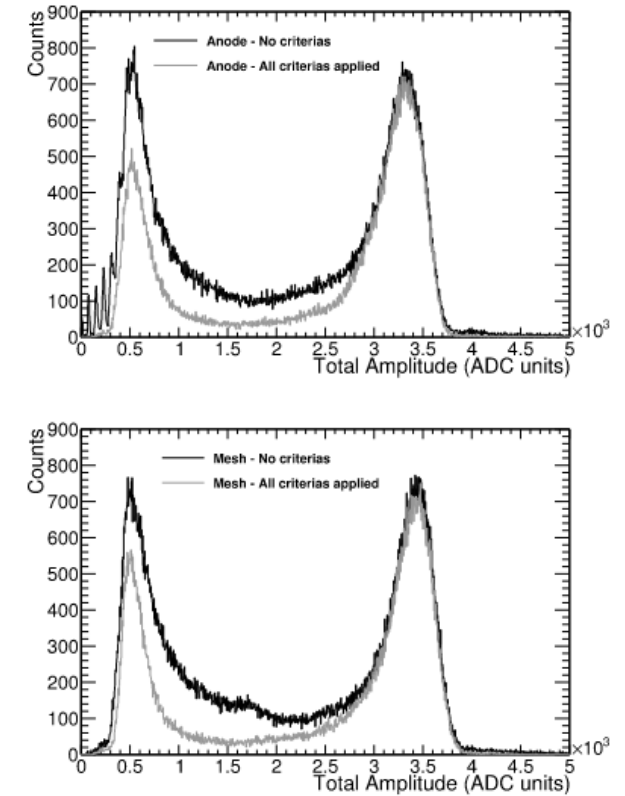


Fig. 11. Reconstructed total amplitude distribution histogram, by adding the amplitudes of all the strip signals in each event, for the anode (up) and the mesh (down), from all the events (black) and only from the selected ones with the criteria applied (grey).

Table 2

Characteristics of the masks used. In most cases, PMMA plates were used in order to reduce the neutron fluence (by a factor of 16).

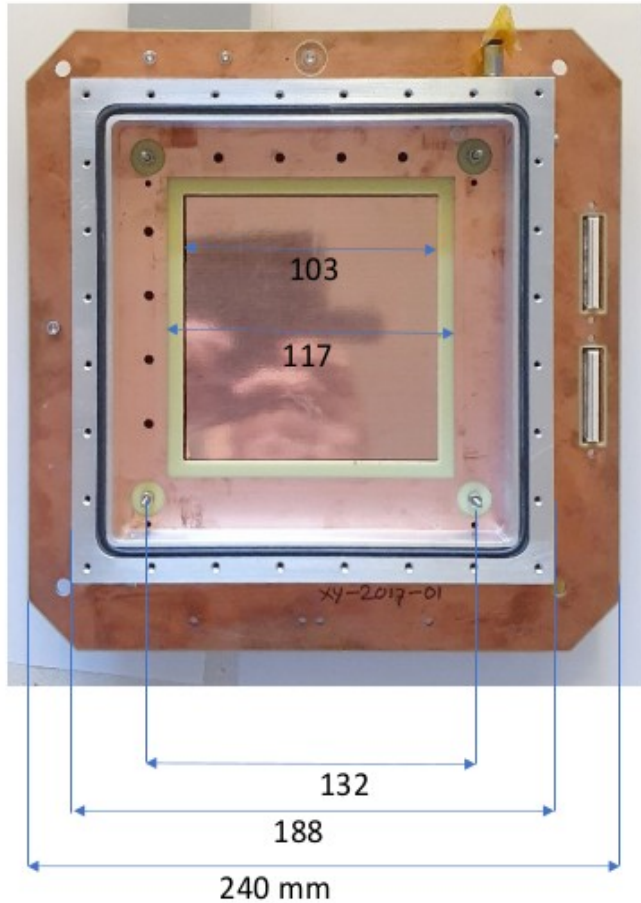
Mask shape	Dimensions (mm)
Circular hole	$\varnothing 5$
Circular hole	$\varnothing 2$
Square hole	$5 \times 5$
Rectangular hole	$1 \times 5$

Development of a novel segmented mesh MicroMegas detector for neutron beam profiling,  
<https://doi.org/10.1016/j.nima.2018.06.019>, Nuclear Inst. and Methods in Physics Research, A 903 (2018) 46–55

# New XY-mmegas design

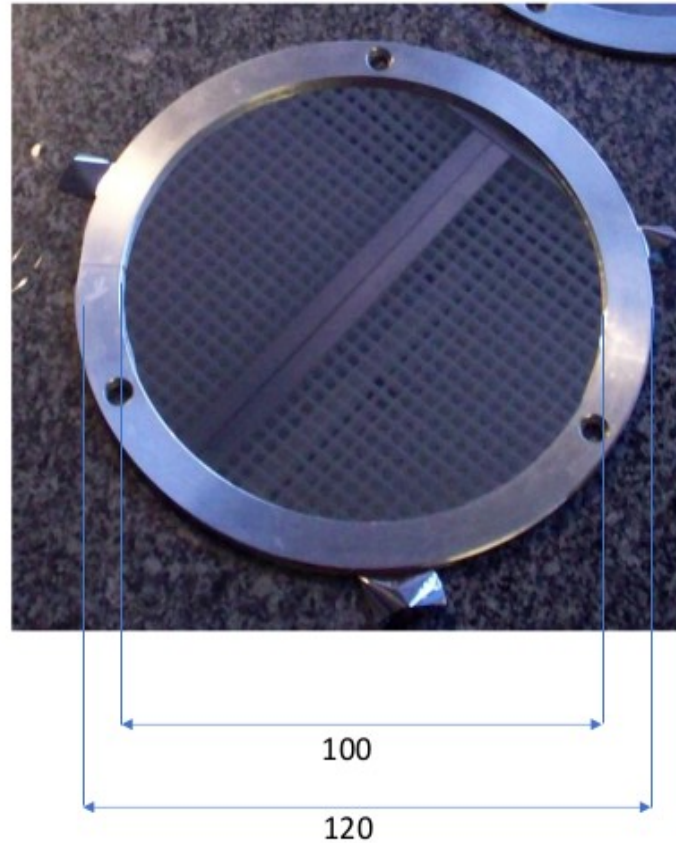
10 x 10 cm<sup>2</sup>

Micromegas chamber



Ar-iC<sub>4</sub>H<sub>10</sub> (5%), 1 Atm

drift, ring Al 1 mm thick, <sup>10</sup>B deposit on mylar 10 μm



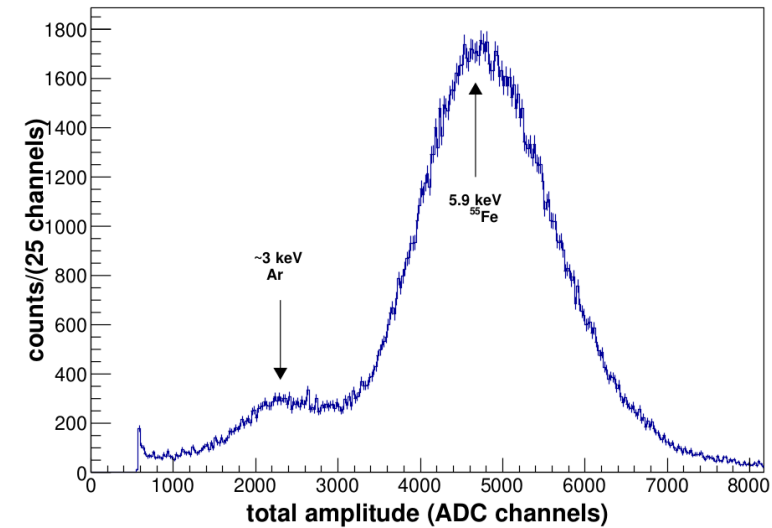
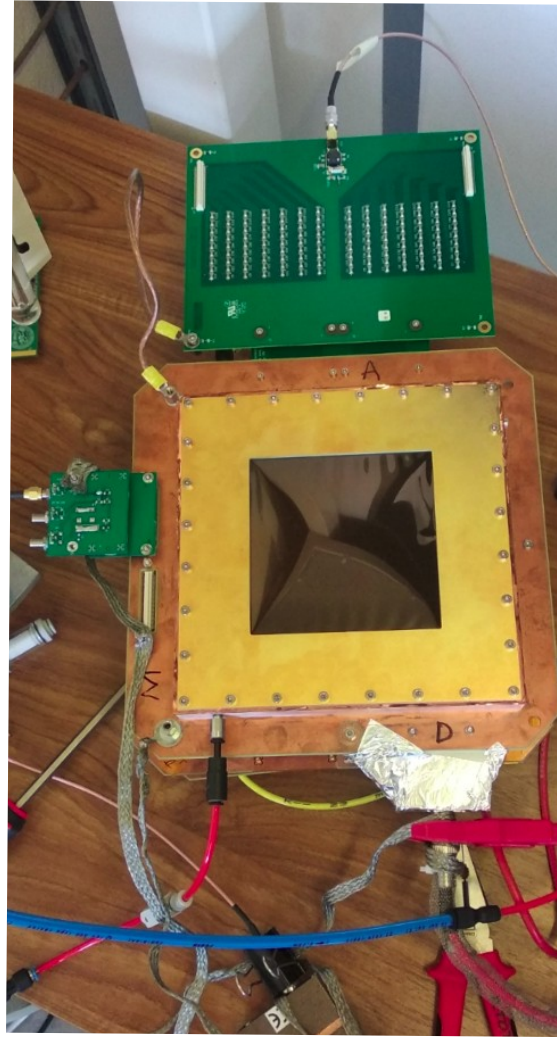
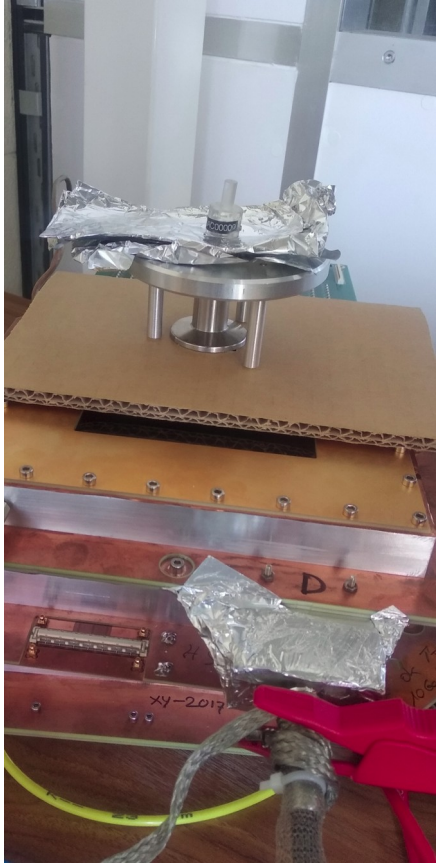
- 100 x 100 strips (10x10 cm<sup>2</sup>)
- Mesh hole ~ 60 μm
- Pitch: 100 μm

- Larger detector
- VMM3 electronics to replace AGET

- n\_TOF facility (CERN) (thermal-GeV)
- GELINA (IRMM) (1meV-20MeV)
- NFS (GANIL) (1-40MeV)



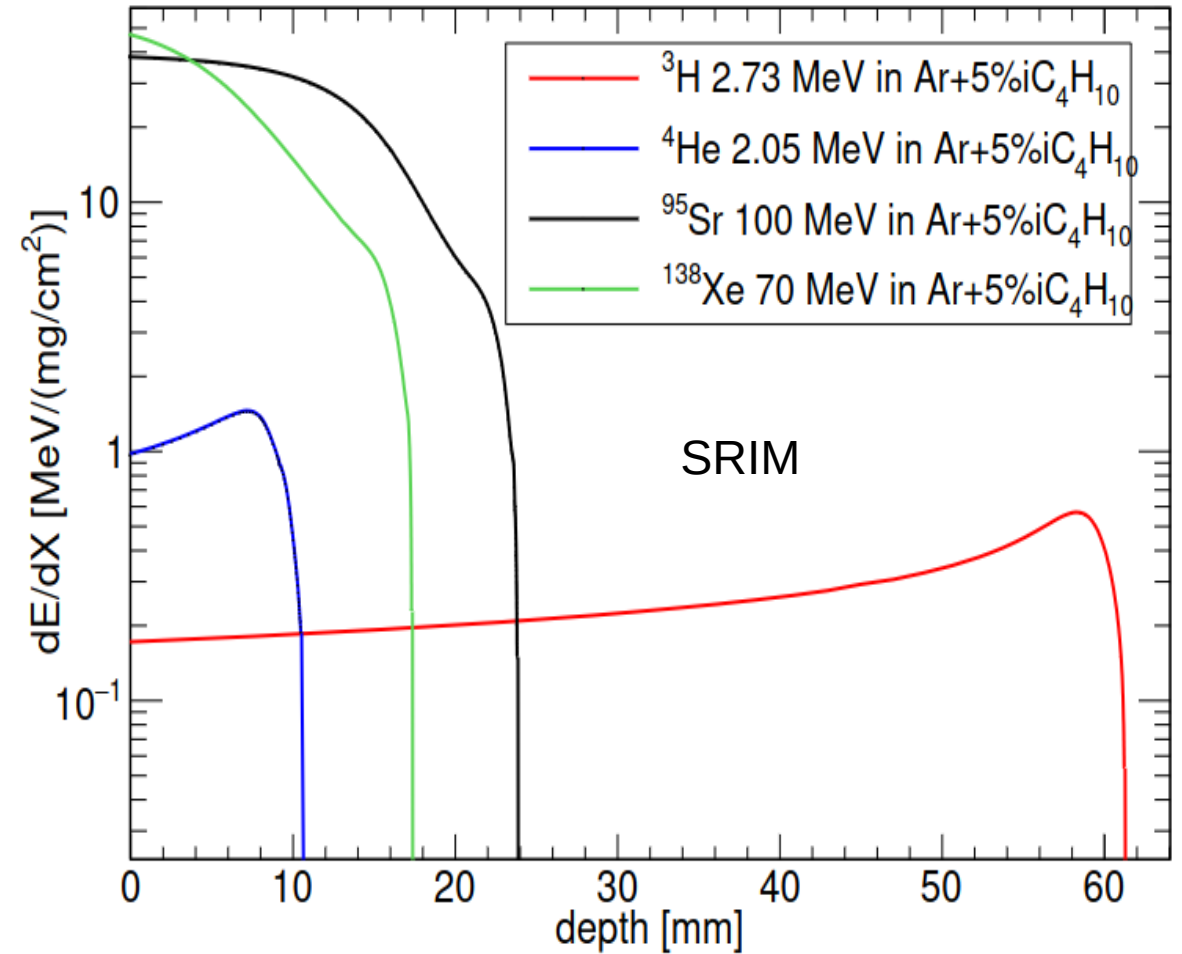
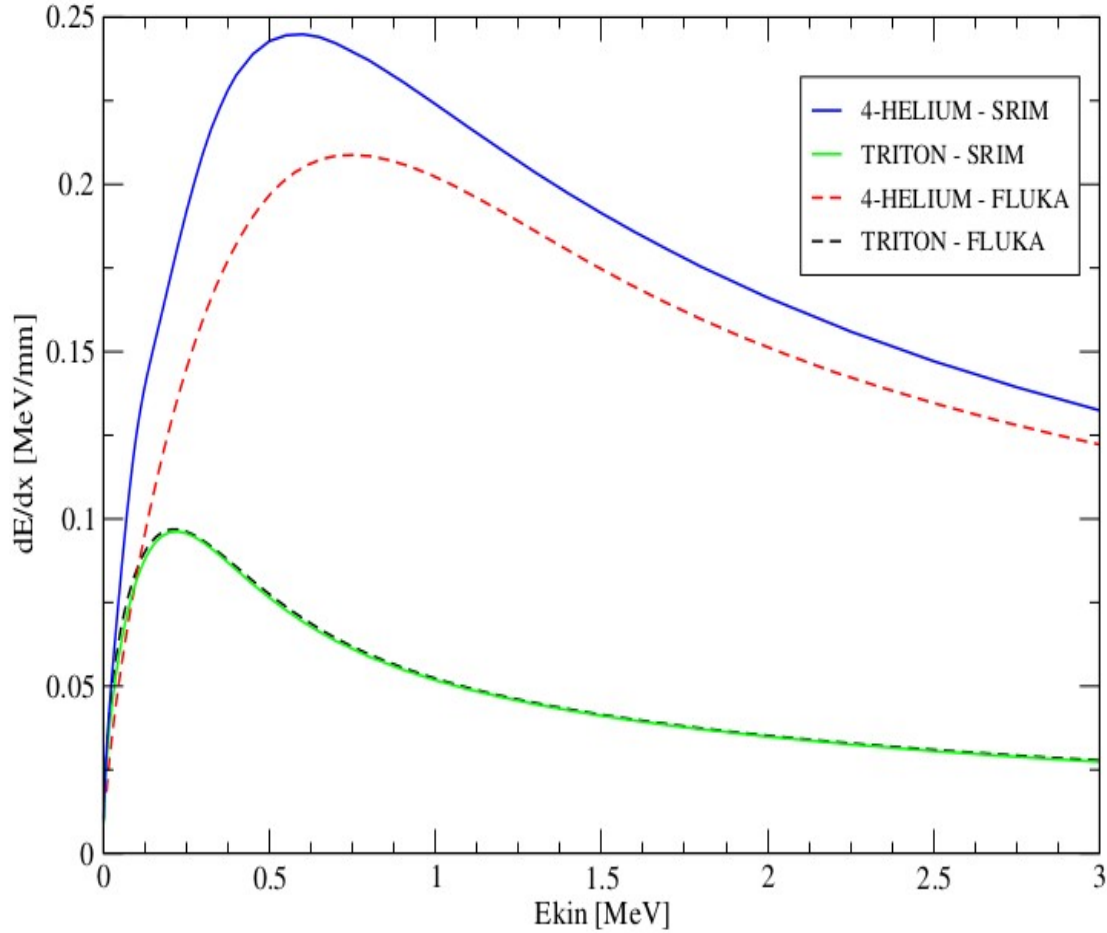
# Experimental set-up and first tests



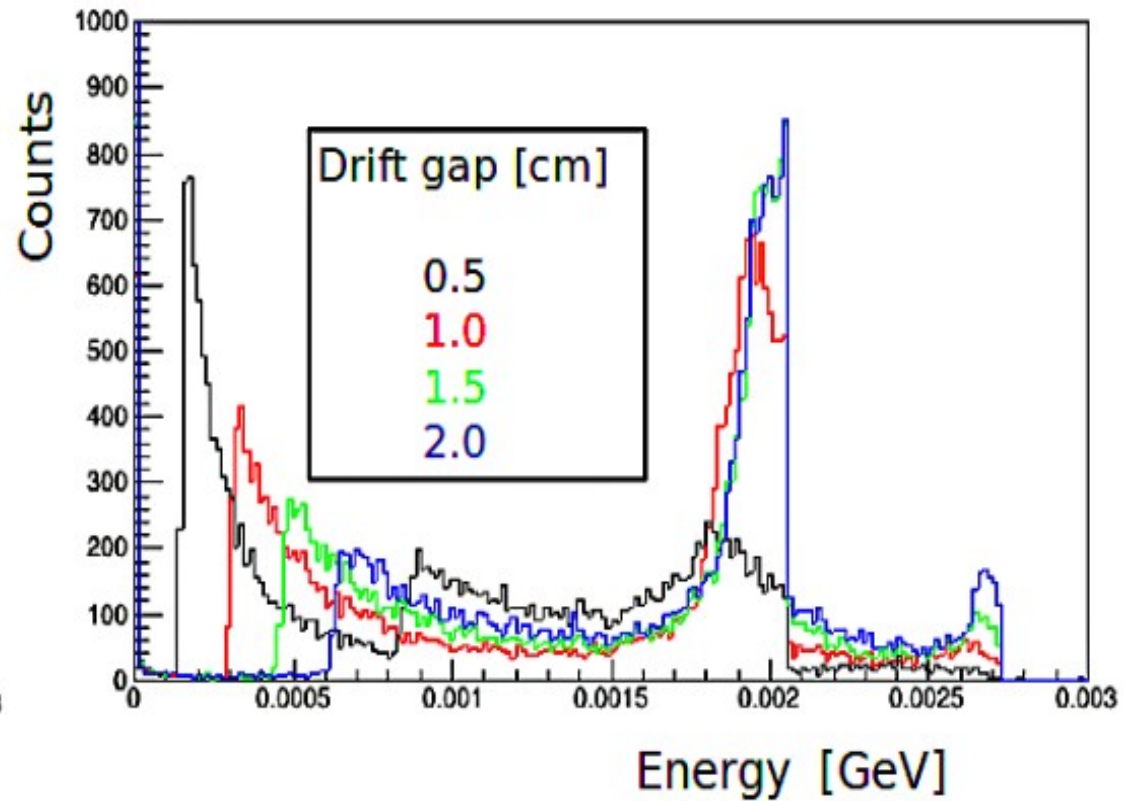
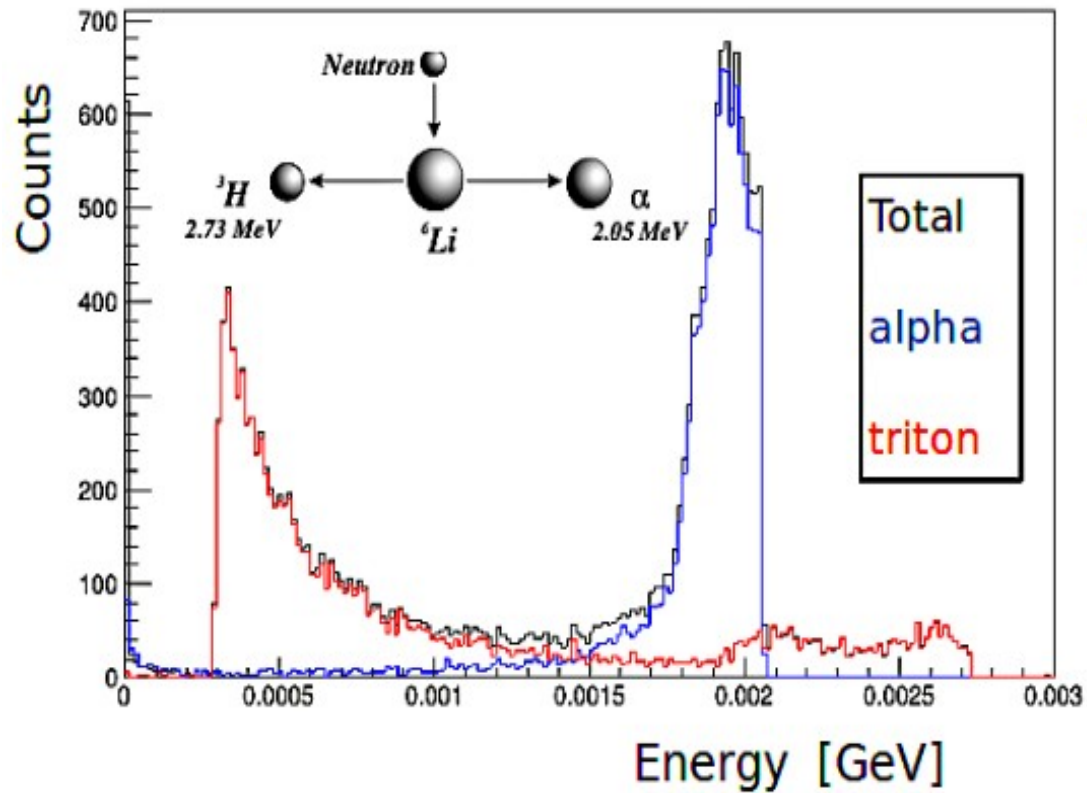


# Penetration depth - SRIM calculations

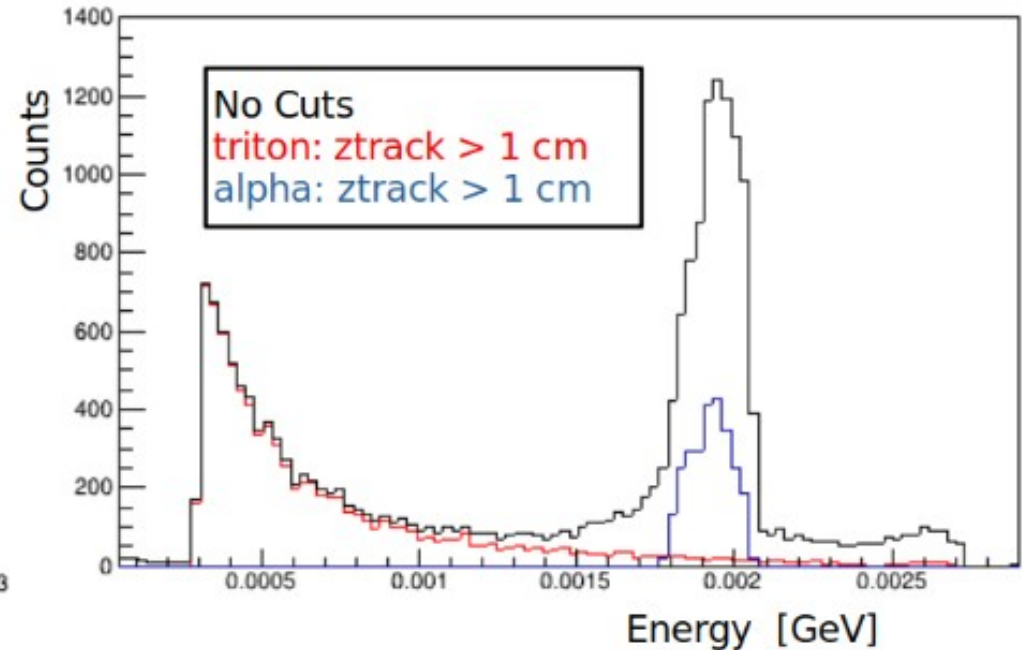
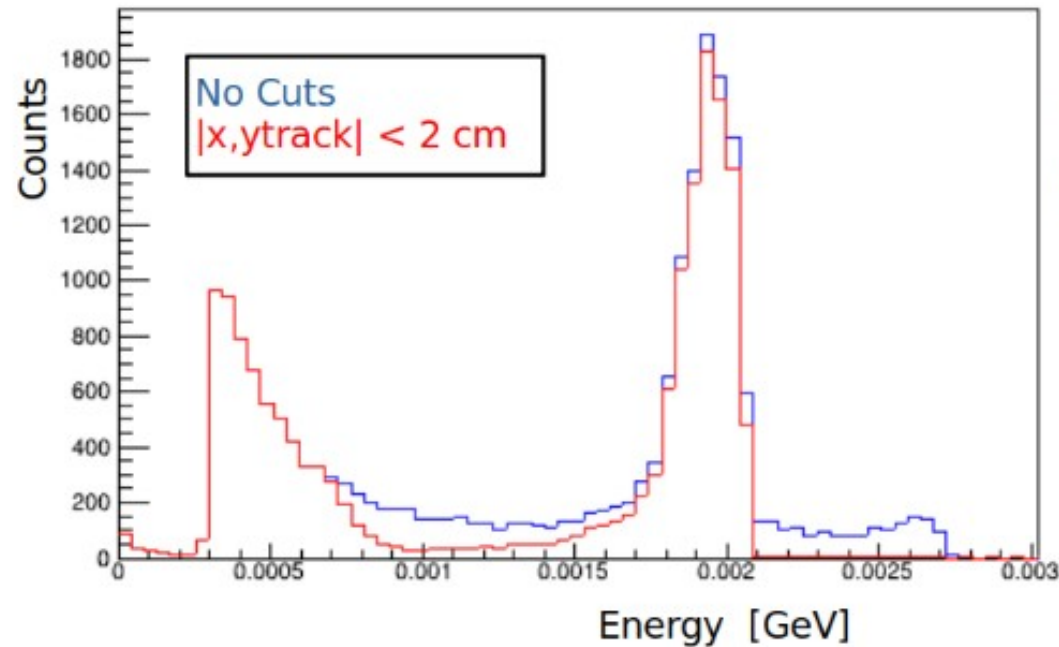
FLUKA vs SRIM



# Energy deposition spectra – FLUKA simulations (i)



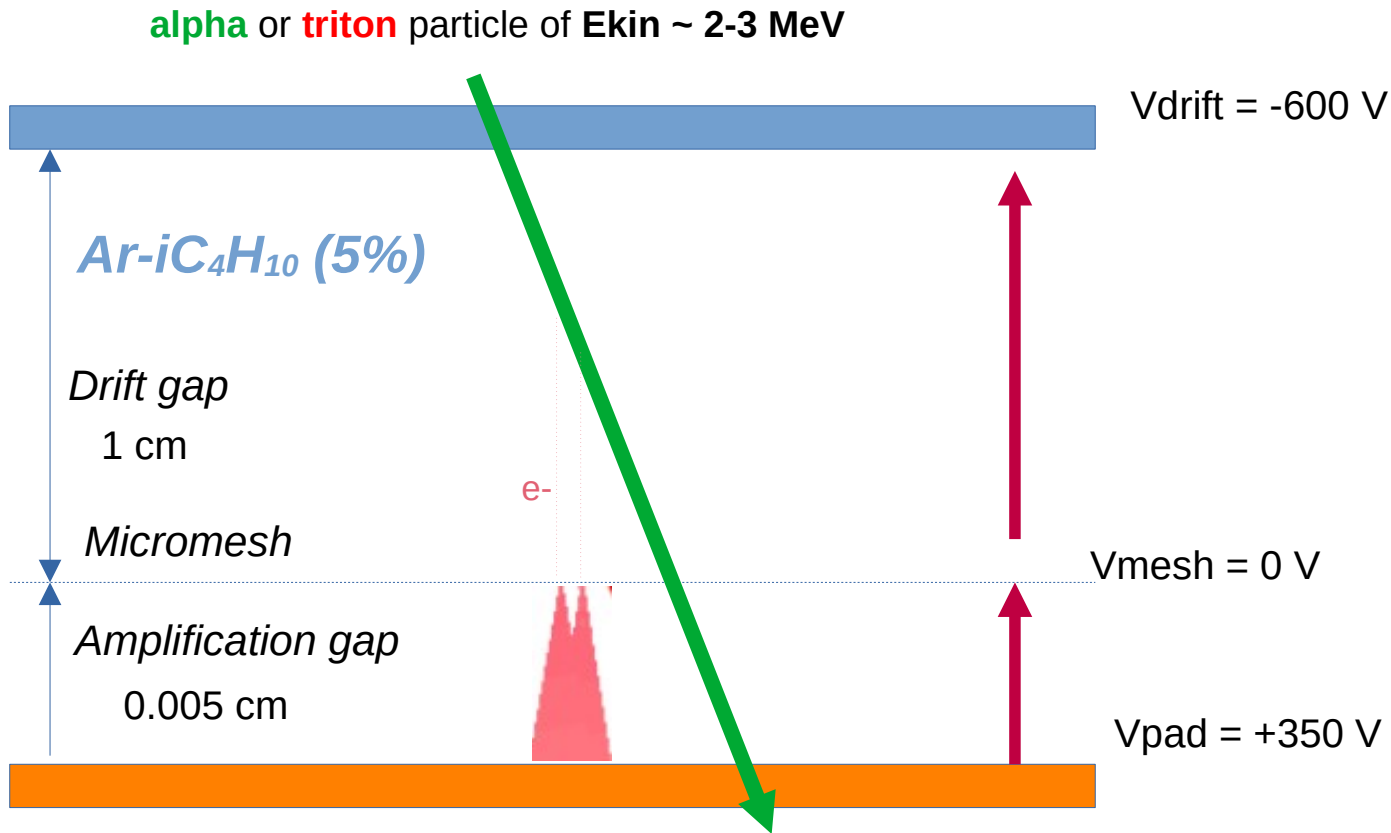
# Energy deposition spectra – FLUKA simulations (ii)



BUT not possible:

- to apply electric fields
- diffusion evaluation
- signal representation etc...

# Garfield++ simulation of micromegas



In Ar, for creation of 1 pair e-/ion  
 $\rightarrow W=26 \text{ eV}$  (work function)  
 Alpha of 2 MeV  $\rightarrow 2 \text{ MeV} / 26 \text{ eV} = 7.7\text{E}+4$  pairs.

$C = \epsilon A / d = 8.85 \text{ pF}$   
 $A = 100 \text{ cm}^2$   
 $d = 1 \text{ cm}$   
 $\epsilon = 8.85\text{E}-12 \text{ F/m}$

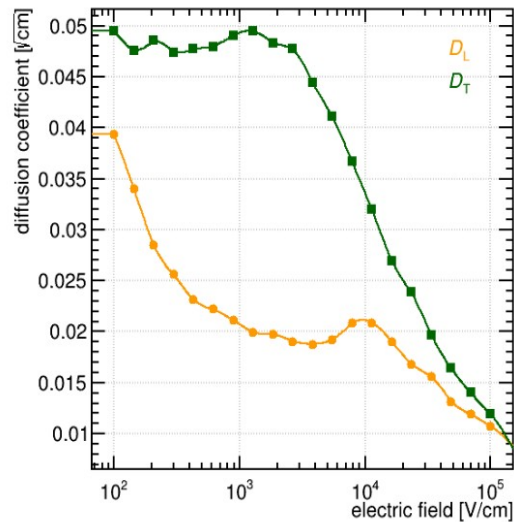
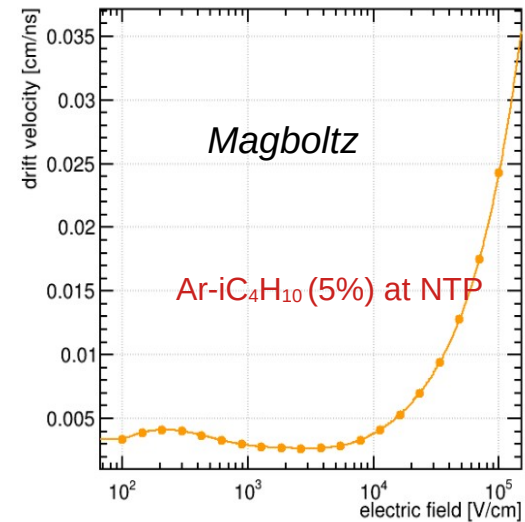
$V = 7.7\text{E}+4 \text{ ions} \times 1.6\text{E}-19 \text{ Cb/ion} / 8.85\text{E}-12 \text{ F} \sim 1.4 \text{ mV}$

physical quantity	unit
length	cm
mass	g
time	ns
temperature	K
electric potential	V
electric charge	fC
energy	eV
pressure	Torr
electric field	V / cm
magnetic field	Tesla
electric current	fC / ns
angle	rad

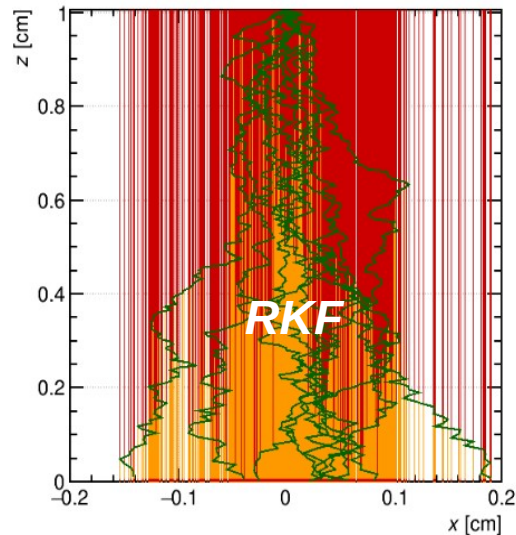
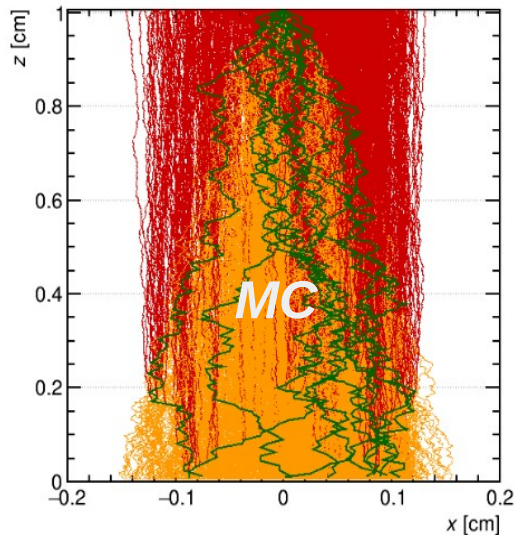
<https://garfieldpp.web.cern.ch/garfieldpp/>



# Garfield++: methods to be used



10 alpha vertical tracks with energy of 2 MeV



→ **DriftLineRKF** calculates the path of an electron or ion by numerical integration of the drift velocity vector. In the absence of a magnetic field, the drift lines will follow the electric field lines (using the previously computed tables of transport parameters to calculate drift lines and multiplication). The method is well adapted to fields that are smooth, such as analytic potentials.

→ **AvalancheMicroscopic** simulates electron trajectories using a “microscopic” Monte Carlo simulation based on the electron-atom/molecule scattering cross-sections where the electron is followed from collision to collision. Provides an accurate simulation of event-by-event fluctuations of the electron signal (very time consuming).

→ **AvalancheMC**, similarly as DriftLineRKF, uses the macroscopic drift velocity as function of the electric field for calculating electron or ion drift lines but adds a random diffusion component to each drift line step. It simulates all electrons in an avalanche individually.

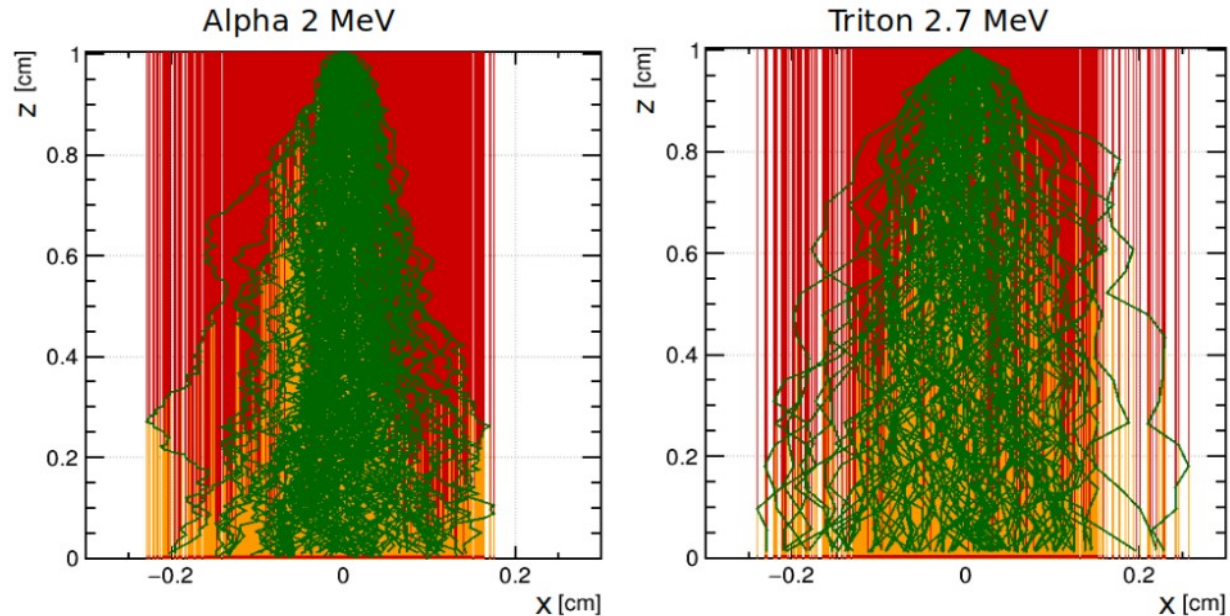
- **DriftLineRKF**: there is no random/Monte Carlo element in the drift line simulation. For a given starting point, all electrons/ions will go at the same end point. On the other hand, **microscopic** tracking of electrons is typically used when fluctuations are important (for instance, when an accurate description of diffusion is needed, especially in non-uniform fields, or for studies of gain fluctuations in the avalanche gap to get the ion signal). For the electrons in the drift gap, diffusion will just spread the arrival points of the electrons at the mesh. In this case, we are looking at the signal induced on the mesh plane as a whole.

- Both methods are used and compared with each-other

→ For a single alpha track:  $\Delta T_{RKF} / \Delta T_{MC} \sim 1 / 4000$  s

# MC vs RKF

2D x-z projection of 100 tracks – RKF

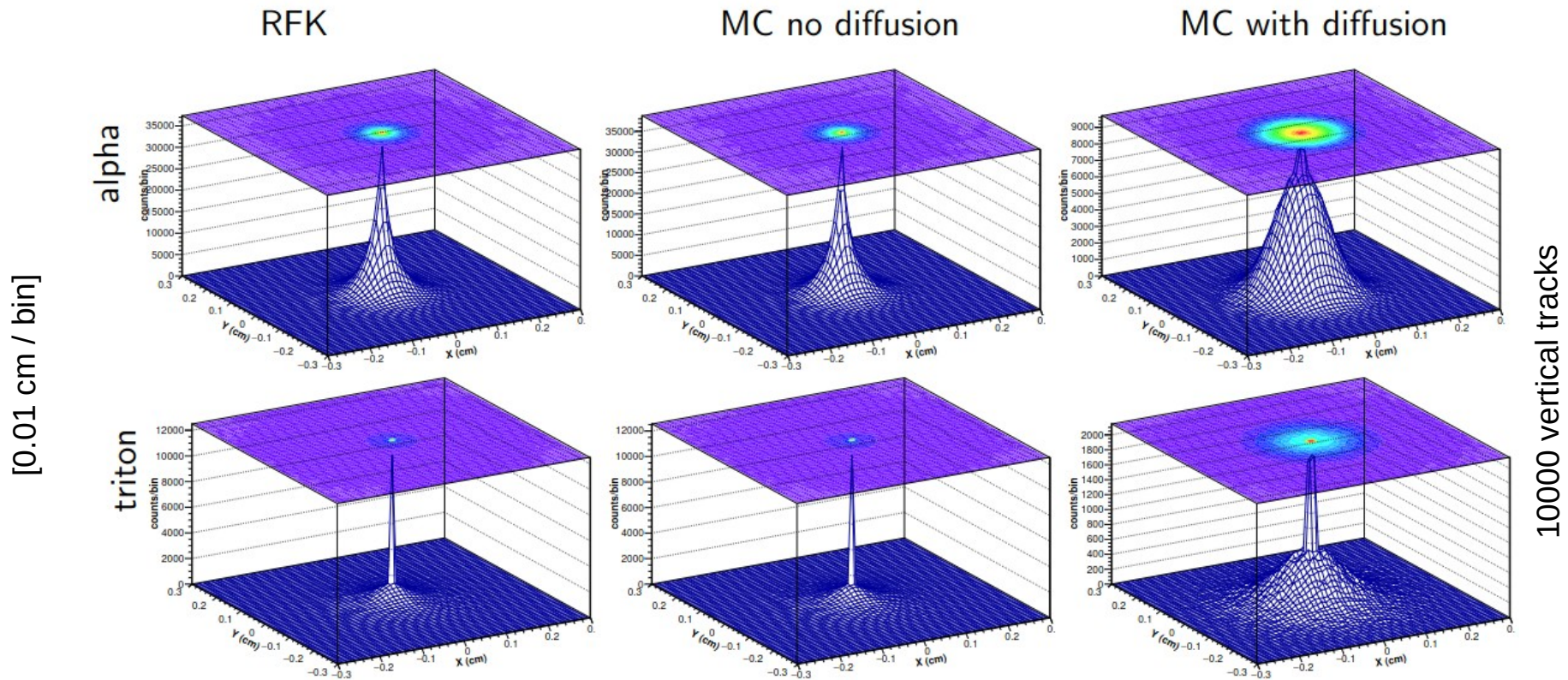


- Generation of 200 vertical 2 MeV  $\alpha$ -particles and 2.7 MeV tritons with Garfield++ with both methods
- Collection of simulated data for the deposited charge in the anode electrode (pad) using the RKF method
- The information for the energy loss for both ionizing particles is obtained by using the SRIM code (version: SRIM-2013.00)
- Load a file with the mobility of the ions in argon
- Then, retrieving the "clusters" along the track, the drift is simulated for each of the primary electrons
- The drift lines of the electrons released in the drift gap will stop once they hit the mesh plane
- Use of the MC method for evaluation of the spread of the arrival points of the electrons in the mesh and estimation of the magnitude of the diffusion

- 200 vertical tracks of 2 MeV  $\alpha$ -particles and 2.7 MeV tritons were tested using both methods
- Both methods produce the same number of primary electrons that are  $\sim 152$  / alpha track and  $\sim 24$  / triton track, while The secondary electrons produced by the microscopic MC method are  $\sim 75.3$  K / alpha track and  $\sim 11.6$  K / triton track
- Are in perfect agreement with the expected quantities of electron—ion pair
- The standard deviations of the distributions of the arrival positions in the XY end plane of the primary electrons as well as of all electrons are almost equal
  - **Using the MC method but tracking only the primary electrons without the tracking of the secondaries**

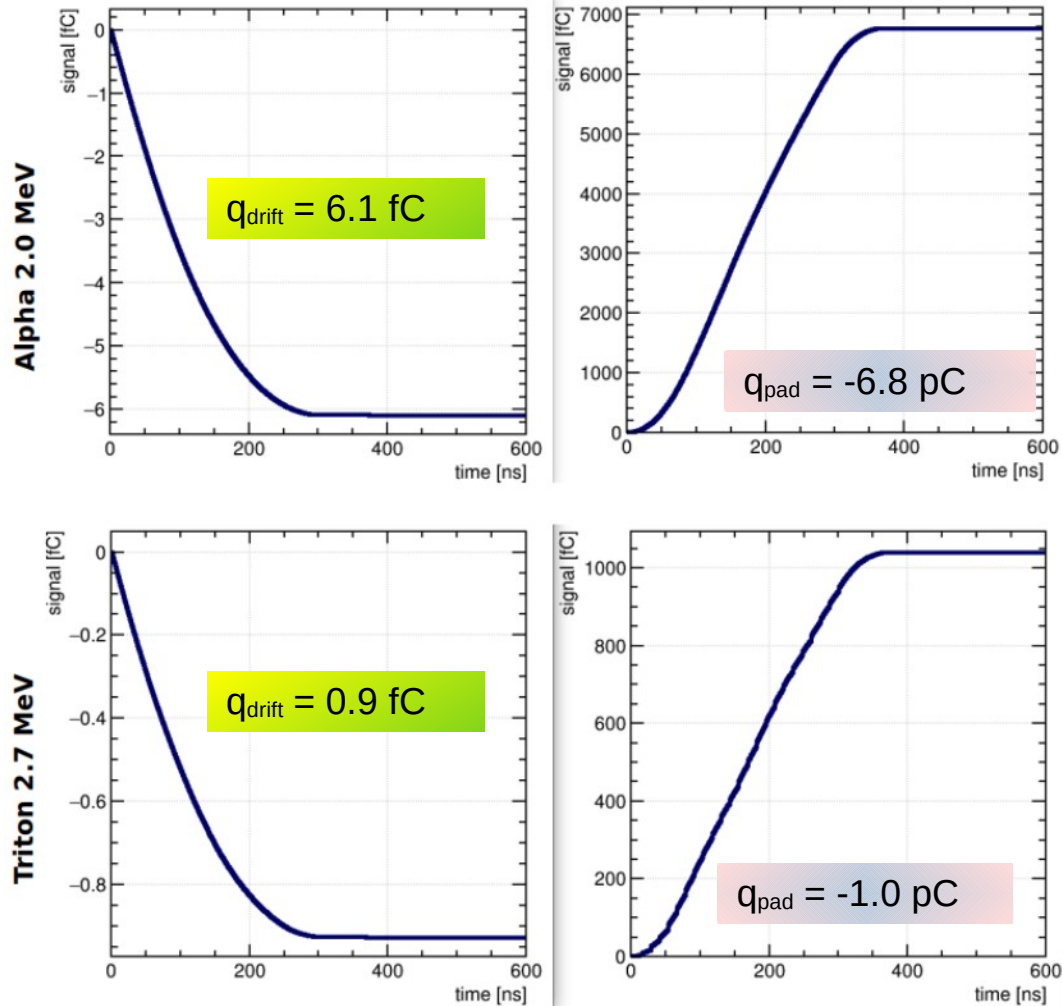


# Comparing RKF and MC: results



Method	RKF	MC no diffusion	MC with diffusion
$\sigma_{\text{alpha}}$ (mm)	0.46	0.46	0.57
$\sigma_{\text{triton}}$ (mm)	0.70	0.70	0.77

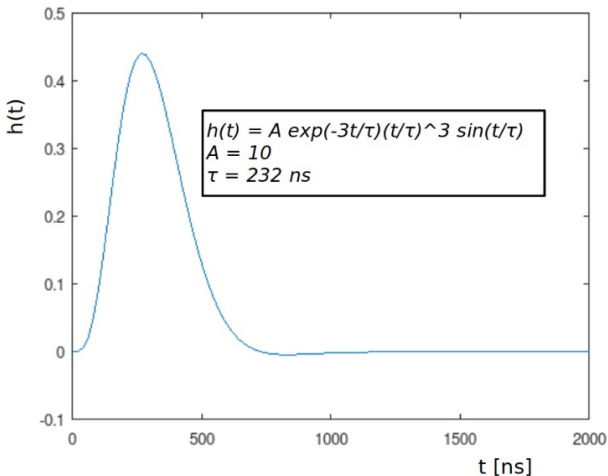
# Simulated total induced charge



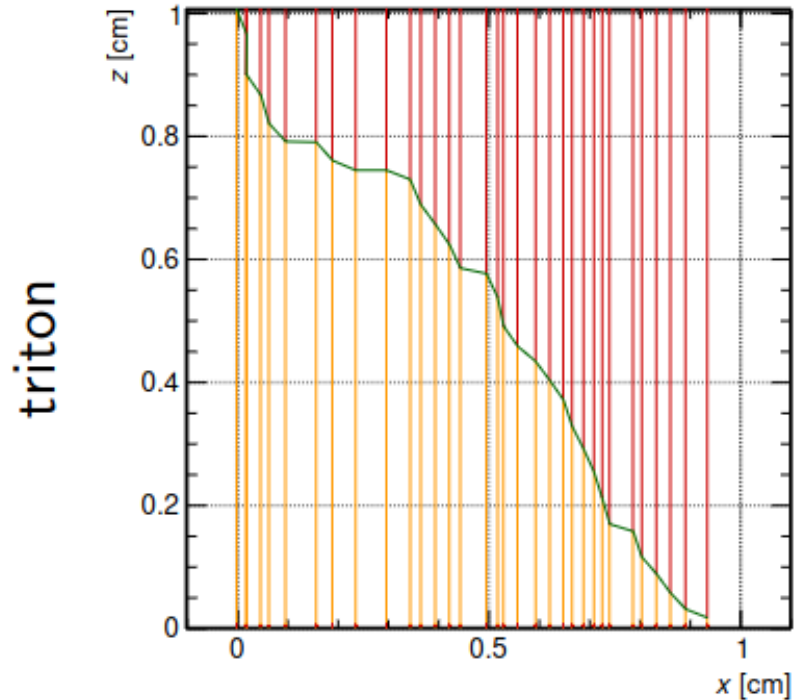
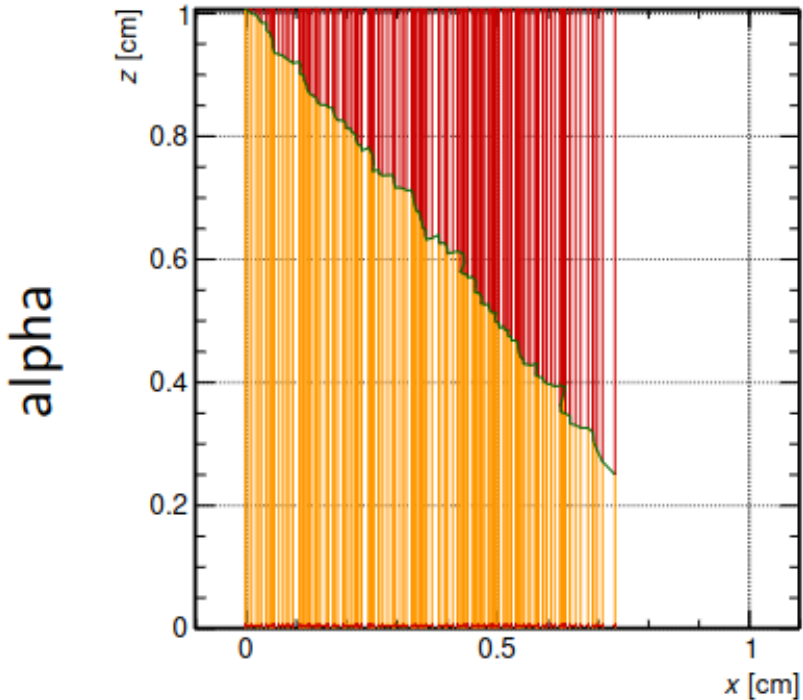
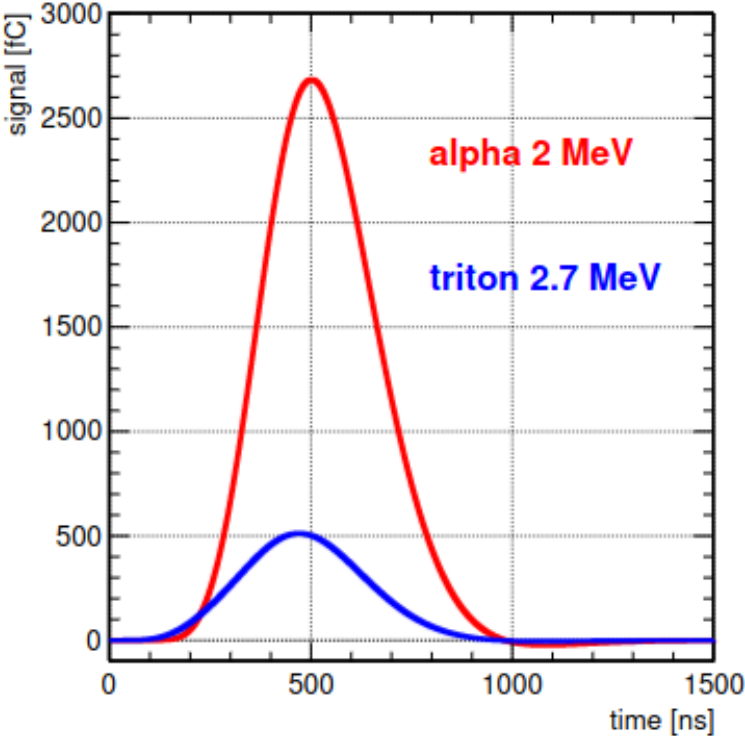
The integral of the induced current pulse related to the total induced charge without any convolution yet with a transfer function for a single vertical alpha / triton track



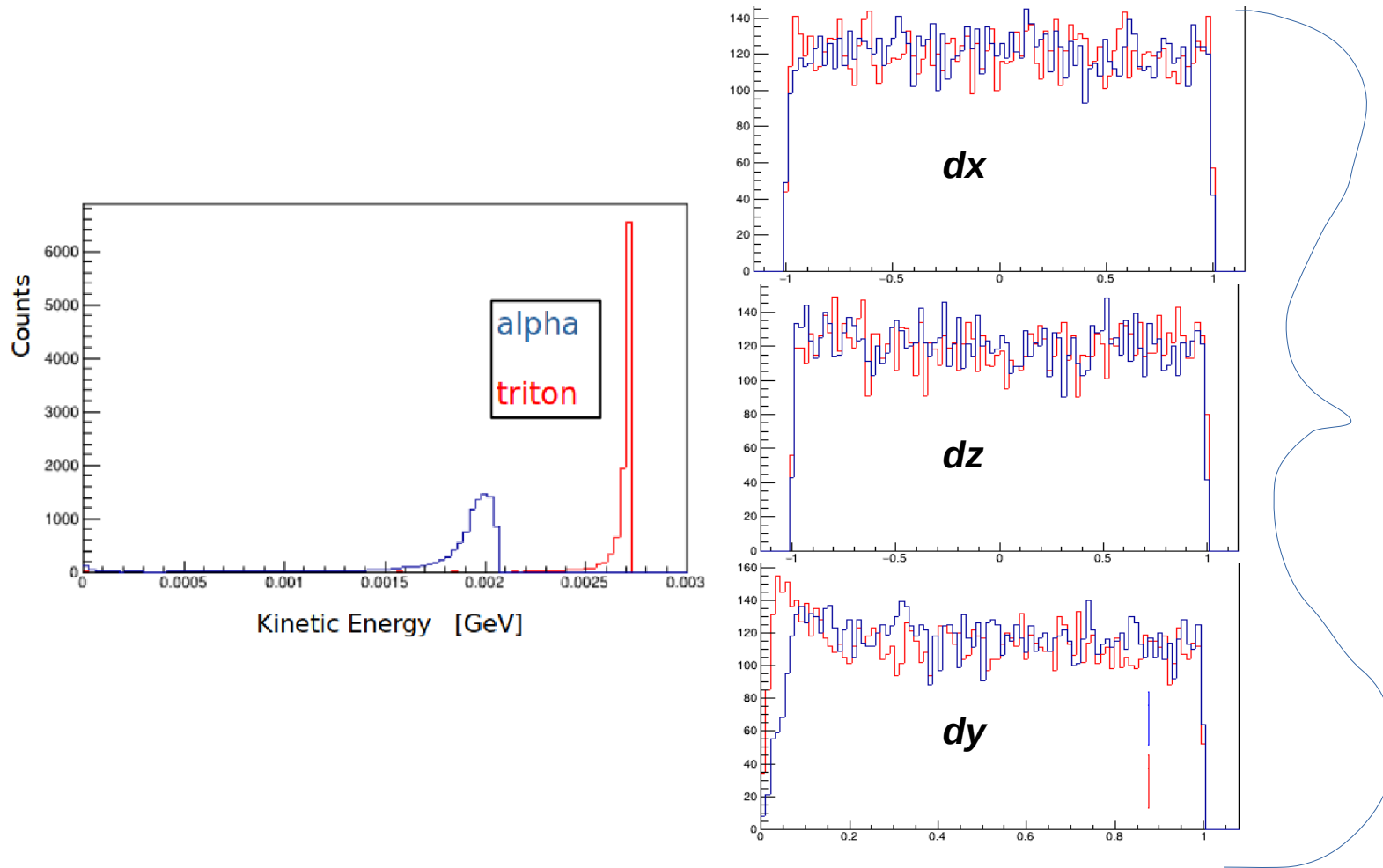
# Pulse after convolution with a GET transfer function



<https://doi.org/10.1016/j.nima.2016.09.018>



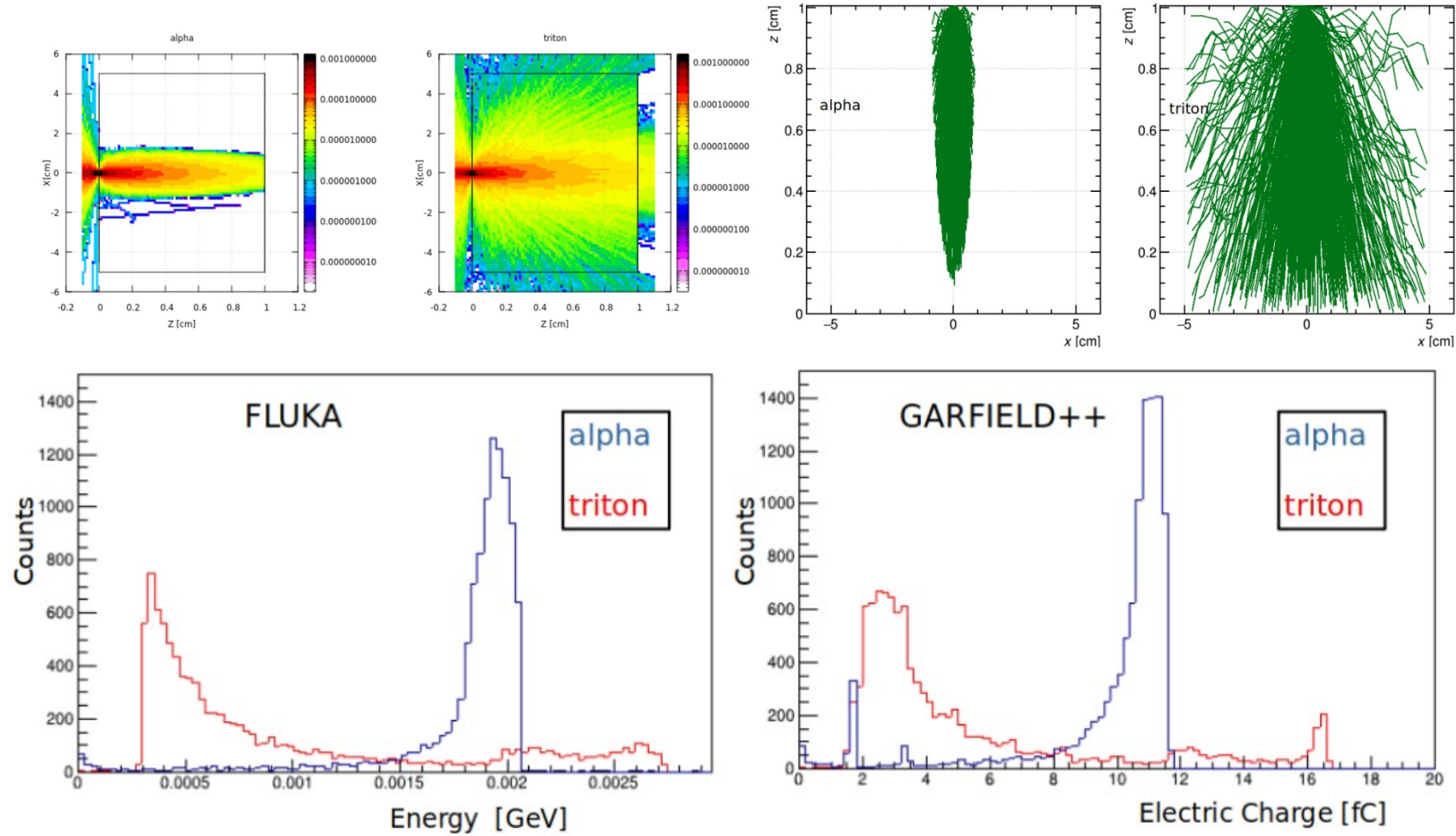
# FLUKA → Garfield++



- Generate a simulated spectrum of  $\alpha$ -particle and triton tracks as exited from the  ${}^6\text{LiF}$  target, having trajectories distributed within the whole detector volume, using Garfield++
- Compare it qualitatively with the simulated total energy deposition histogram as calculated by FLUKA.

Insert  $E_{\text{kin}}$  and direction of alpha and triton ( $\text{LiF} \rightarrow \text{GAS}$ ) from FLUKA to Garfield++

# FLUKA energy deposition spectrum vs RKF deposited charge



~ 10000 alpha / triton tracks

# Summary

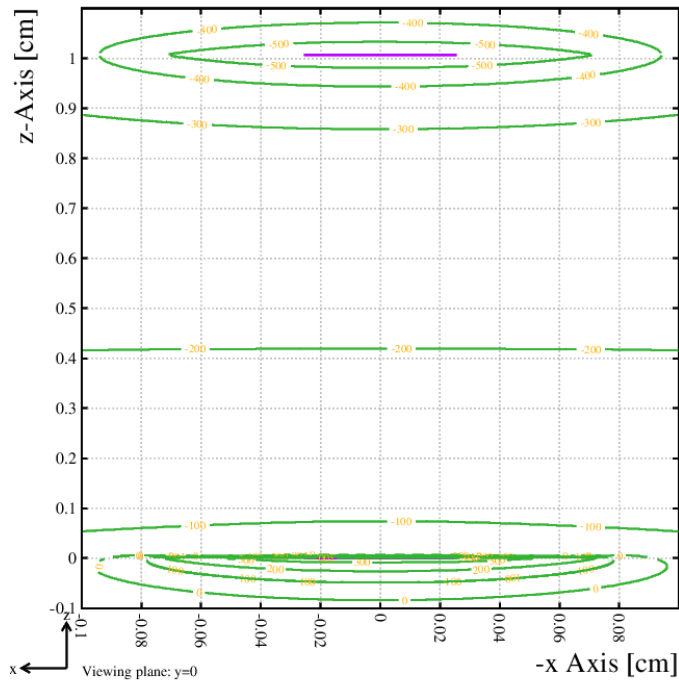
- A solid simulation framework for the XY micromegas detector has been established using the current state-of-the-art MC computer codes FLUKA, Geant4 and Garfield++, SRIM
- Extract at first with a transport MC code (FLUKA, Geant4) the energies and direction cosines of the neutron reaction products and then use Garfield++ to transport them in the drift region and record all the primary electrons that arrive on the micromesh, using the full MC microscopic model enabling only the tracking of primary electrons
- Following this scheme of analysis, we plan to address and carry out studies using other type of converters and fission fragments

# Outlook

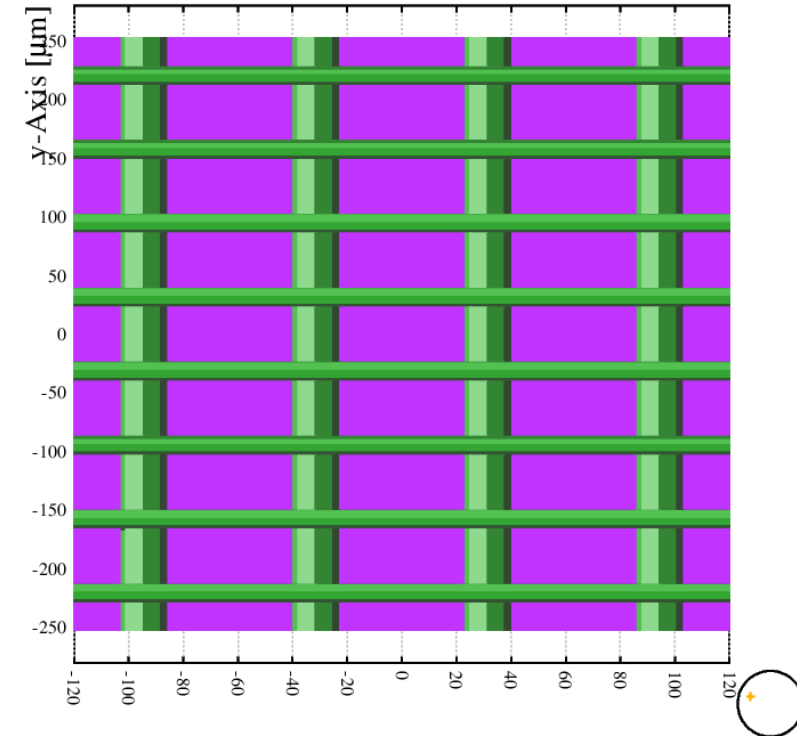
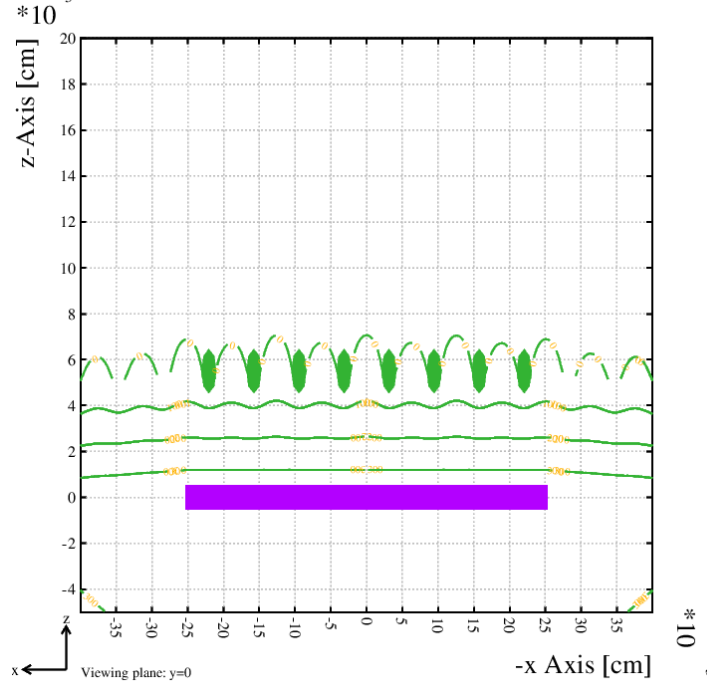


# neBEM / Garfield

Contours of V



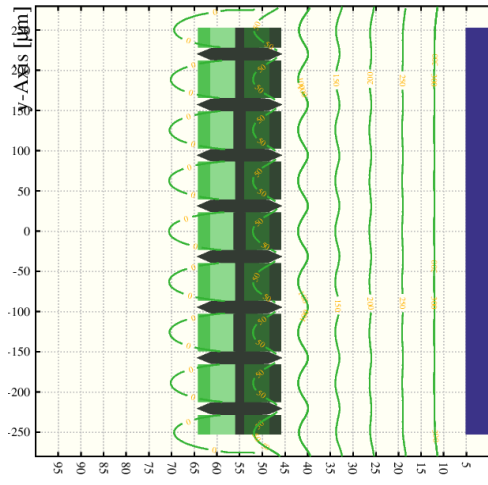
Contours of V



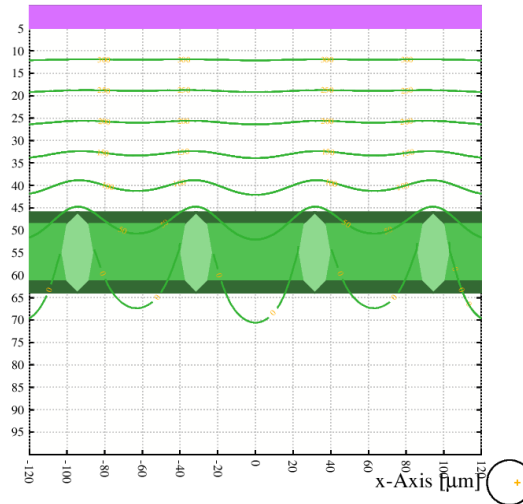
From top to bottom: HV1 = -600, HV2 = 0, HV3 = +350 [V]  
 Wire diameter = 0.0018, Hole diameter = 0.0045 [cm]  
 Drift gap: 1 and Amplification gap: 0.0050 [cm]

# neBEM / Garfield

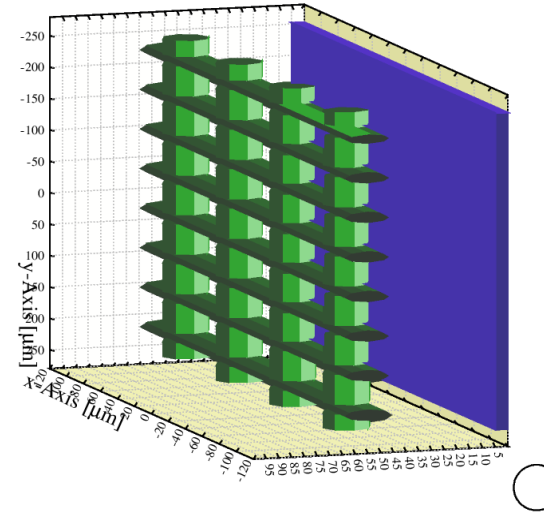
Contours of V



Contours of V

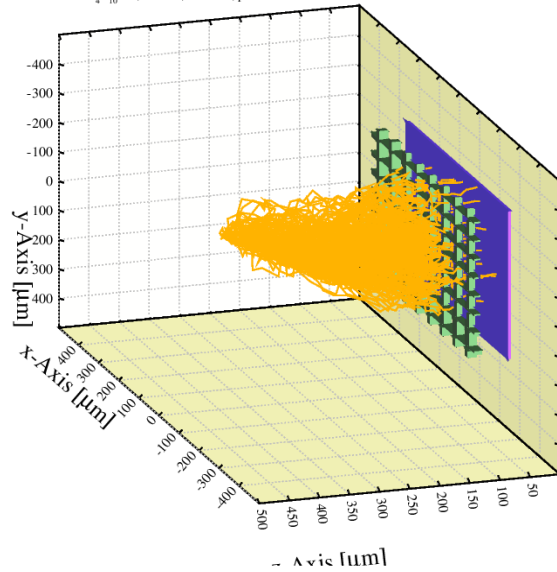


Layout of the cell

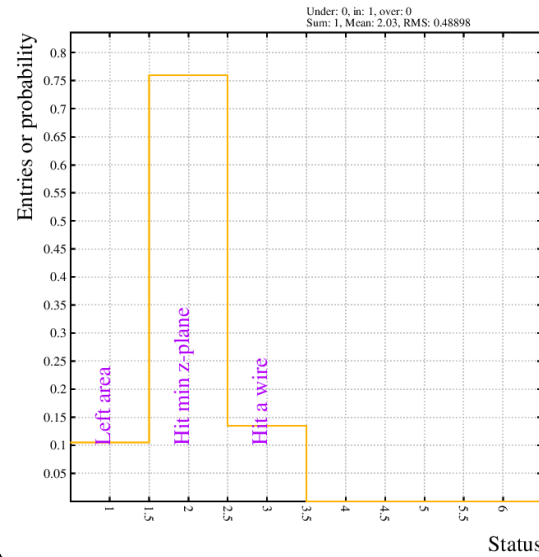


Layout of the cell

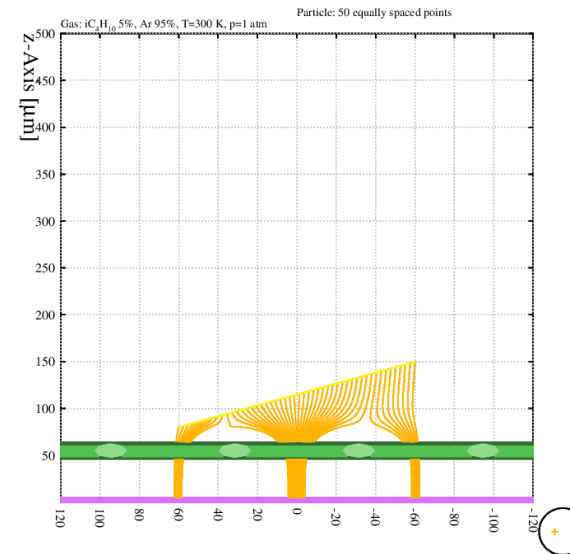
Gas:  $iC_4H_{10}$  5%, Ar 95%, T=300 K, p=1 atm



Fate of electrons

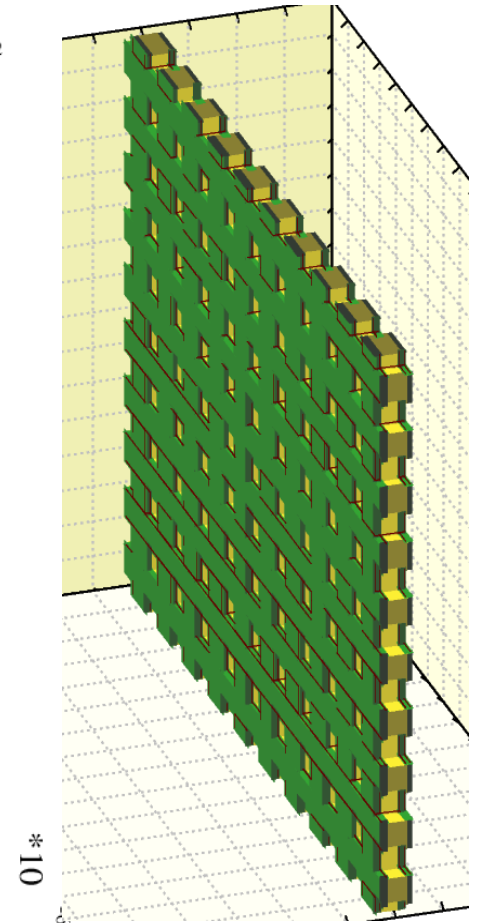
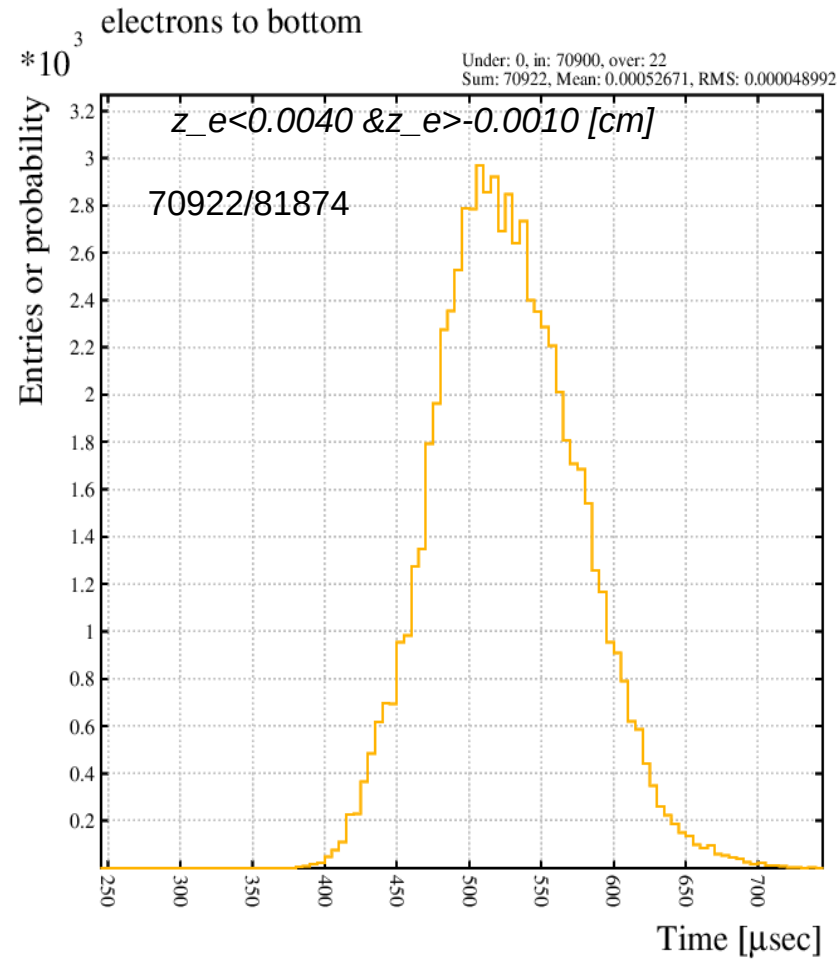
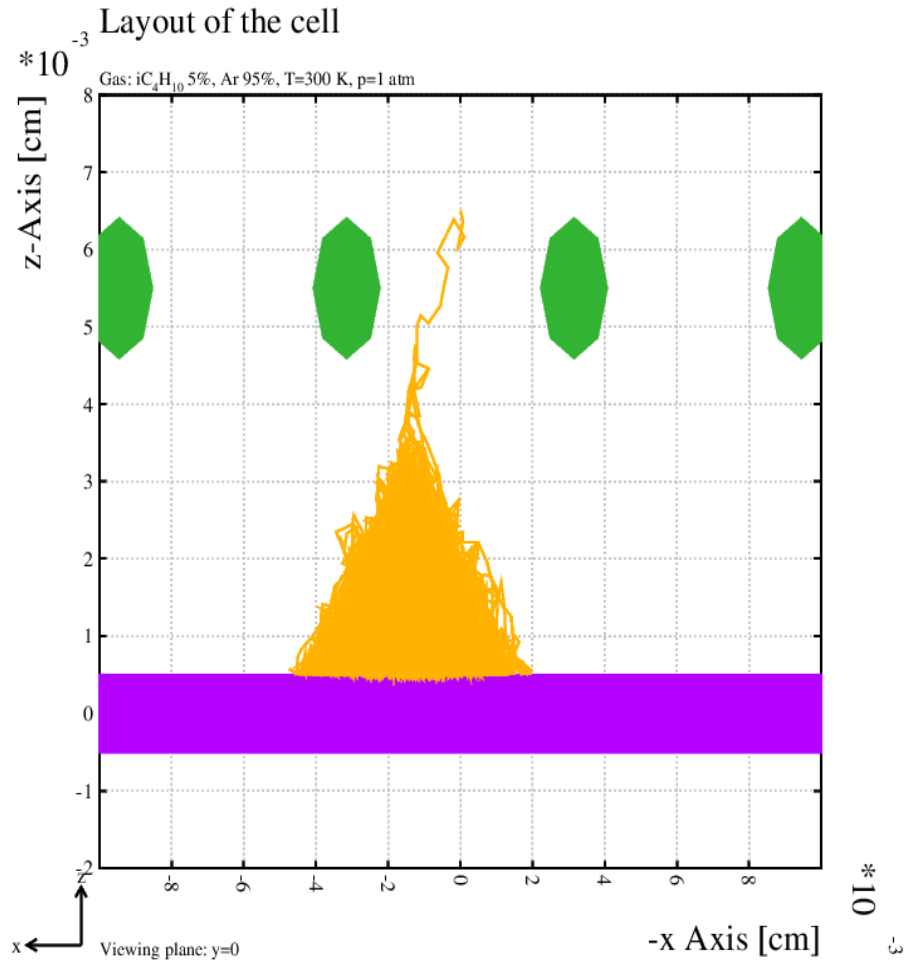


Electron drift lines from a track

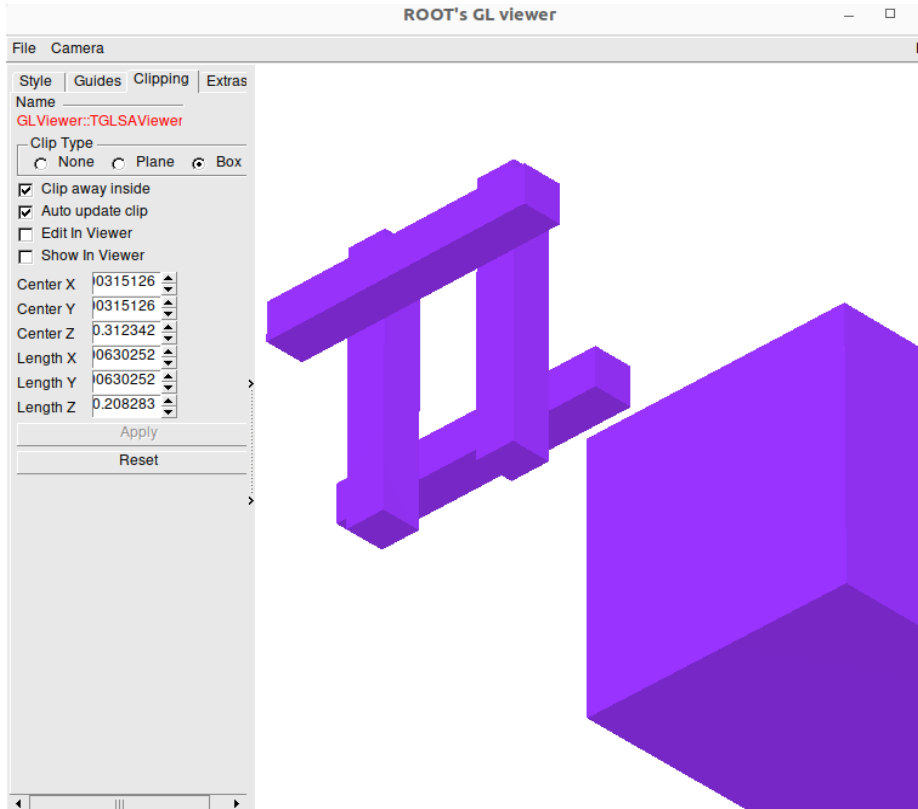


<https://nebem.web.cern.ch/nebem/>

# neBEM / Garfield



# neBEM / Garfield++



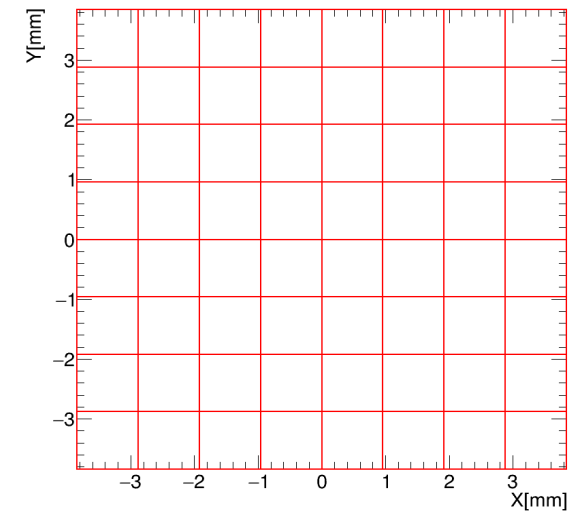
# rest-framework

```
root [0] REST_Detector_ViewReadout("readouts.root", "pixel")
```

```
-----  
TRestDetectorReadout content  
Config file : readouts.rml  
-----  
Name : pixelReadout  
Title : A basic pixel readout 0.96mm-Pitch 8x8 channels  
REST Version : 2.4.0  
REST Official release: Yes  
Clean state: Yes  
REST Commit : 075f65d7  
REST Library version : 2.0  
-----  
Number of readout planes : 1  
Decoding was defined : NO  
-----  
-- Readout plane : 0  
-----  
-- Position : X = 0 mm, Y = 0 mm, Z = 0 mm  
-- Normal vector : X = -0.57735 mm, Y = -0.57735 mm, Z = -0.57735 mm  
-- X-axis vector : X = 0.211325 mm, Y = -0.788675 mm, Z = 0.57735 mm  
-- Y-axis vector : X = -0.788675 mm, Y = 0.211325 mm, Z = 0.57735 mm  
-- Cathode Position : X = -28.8675 mm, Y = -28.8675 mm, Z = -28.8675 mm  
-- Height : 50 mm  
-- Charge collection : 1  
-- Total modules : 1  
-- Total channels : 64  
-----
```

```
(int) 0  
root [1] .q
```

Readout: pixelReadout --- plane: 0

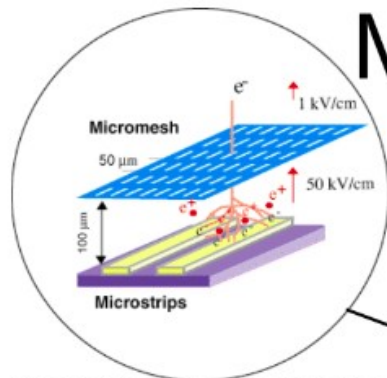


<https://doi.org/10.1016/j.cpc.2021.108281>

back-up



# Micromegas concept



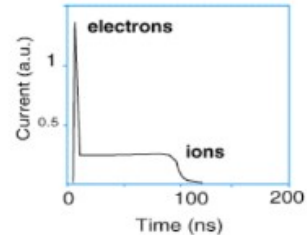
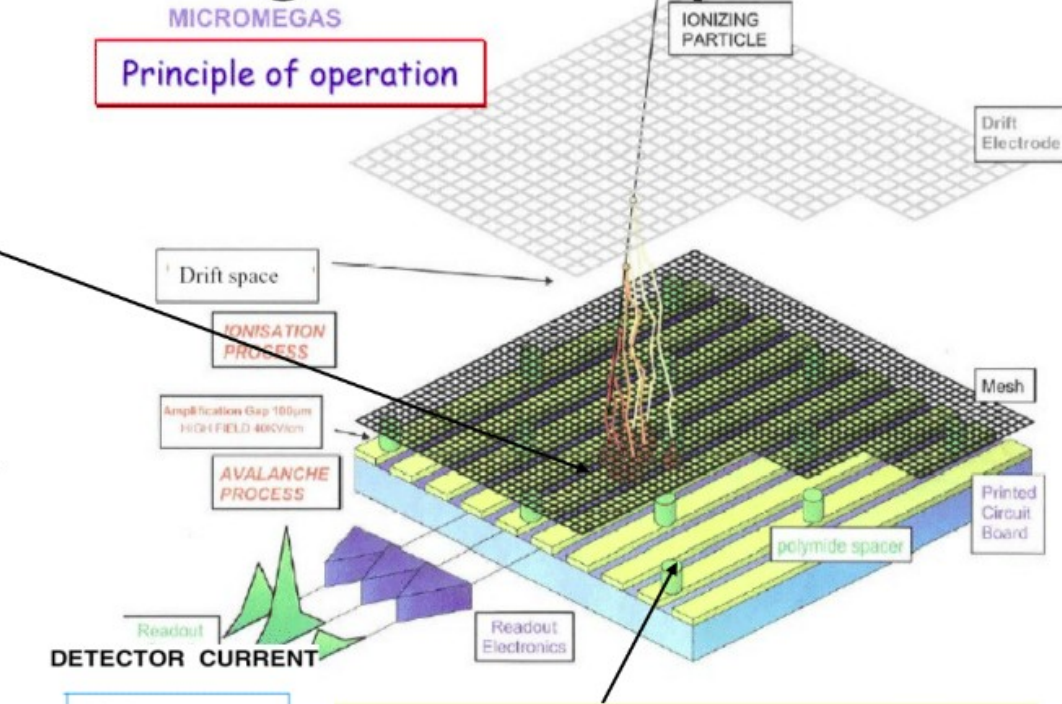
Two-region gaseous detector  
*separated by a Micromesh* :

- Conversion region
  - Primary ionization
  - Charge drift towards A.R.
- Amplification region
  - Charge multiplication
  - Readout layout
  - Strips (1/2 D)
  - Pixels

==>Very strong and uniform E.F.

- simplicity
- single stage of amplification
- fast and natural ion collection
- discharges non destructive

## MICROMEGAS Principle of operation



**keeping the gap constant ~100 μm gap**

- Ni or Cu micromesh + pillars on PCB
- Self-supported copper micromesh
- « bulk » and « micro-bulk » technologies
- Recent InGrid techniques : mesh over Si pixel chip

Micro Mesh Gaseous Structure, Y. Giomataris, Ph. Rebourgeard, J-P Robert and G. Charpak, NIM A376, 1996, p29 (CEA-biospace patent)



# Neutron detection with Micromegas

Due to the so-called  $^3\text{He}$  shortage crisis, many detection techniques used nowadays for thermal neutrons are based on alternative converters. Thin films of  $^{10}\text{B}$  or  $^{10}\text{B}_4\text{C}$  are used to convert neutrons into ionizing particles which are subsequently detected in gas proportional counters, but only for small or medium sensitive areas so far.

## Neutron detection $\rightarrow$ neutron to charge converter

➤ Solid converter: thin layers deposited on the drift or mesh electrode ( $^{10}\text{B}$ ,  $^{10}\text{B}_4\text{C}$ ,  $^6\text{Li}$ ,  $^6\text{LiF}$ ,  $\text{U}$ , actinides...)

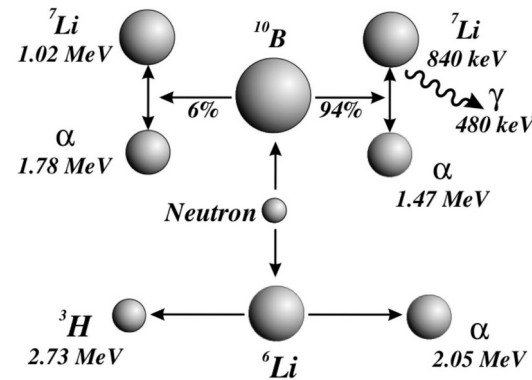
- ✓ Sample availability & handling
- ✓ Efficiency estimation
- ✗ Limitation on sample thickness from fragment range
  - ▲ limited efficiency
- ✗ Not easy to record all fragments

➤ Detector gas ( $^3\text{He}$ ,  $\text{BF}_3$ ...)

- ✓ Record all fragments
- ✓ No energy loss for fragments ▲ reaction kinematics
- ✓ No limitation on the size ▲ high efficiency
- ✗ Gas availability
- ✗ Handling (highly toxic or radioactive gasses)

➤ Neutron elastic scattering

- gas ( $\text{H}$ ,  $\text{He}$ )
- solid (paraffin etc.)
  - ✓ Availability
  - ✓ High energies
  - ✗ Efficiency estimation & reaction kinematics



## Neutron detection with high efficiency (~50%):

- $^3\text{He}$  crisis
- Increased demand for neutron detectors
  - ➔ Science
  - ➔ Homeland security
  - ➔ Industry

## Micromegas for neutrons

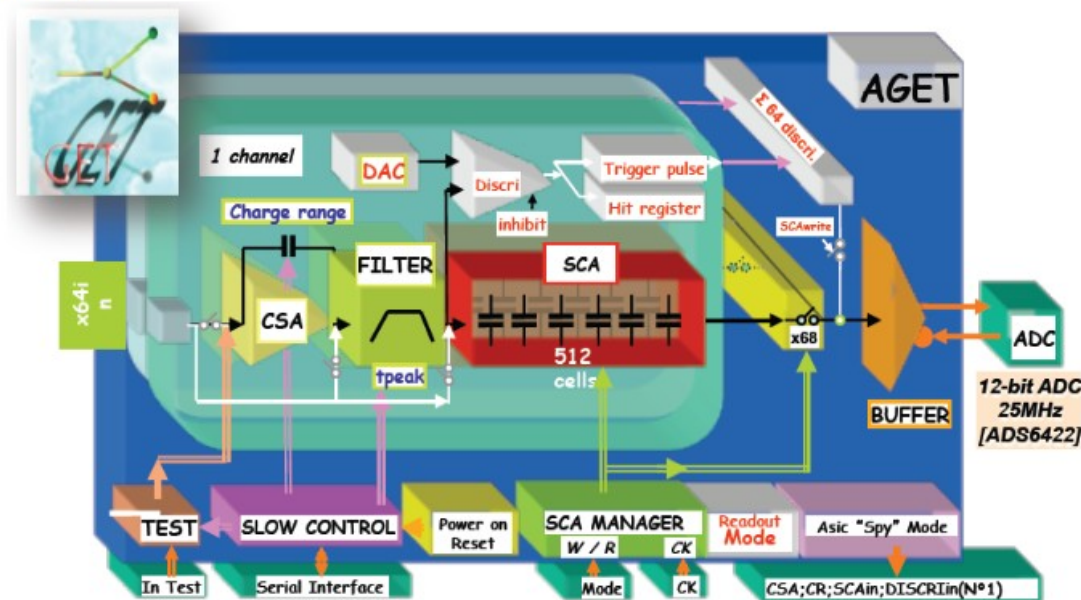
- Micro-Pattern Gaseous Detector (gain, fast timing, high rate, granularity, radiation hardness, simplicity...)
- Low mass budget
- Transparent to neutrons
- Large area detectors cheap & robust



Challenge:

No global trigger signal => **AGET electronics\*** + **Reduced CoBo configuration**  
Self triggering mode / timing difference between strips.

- 64 analog channels /chip.
- Auto trigger: discriminator and threshold
- Multiplicity signal: analog OR of 6discriminators
- Address of the hitted channels
- SCA readout mode (all/hitted/selected channels)
- Max sampling rate: 100 MHz.
- 16 peaking time values: 50 ns-1us.
- 4 charge ranges/channel: 120fC/ 240fC/  
1pC/ 10 pC.



\*GET, General electronics for TPC, ANR proposal / GET-QA-000-0005, AGET Data Sheet.



Accurate neutron cross section measurements require:

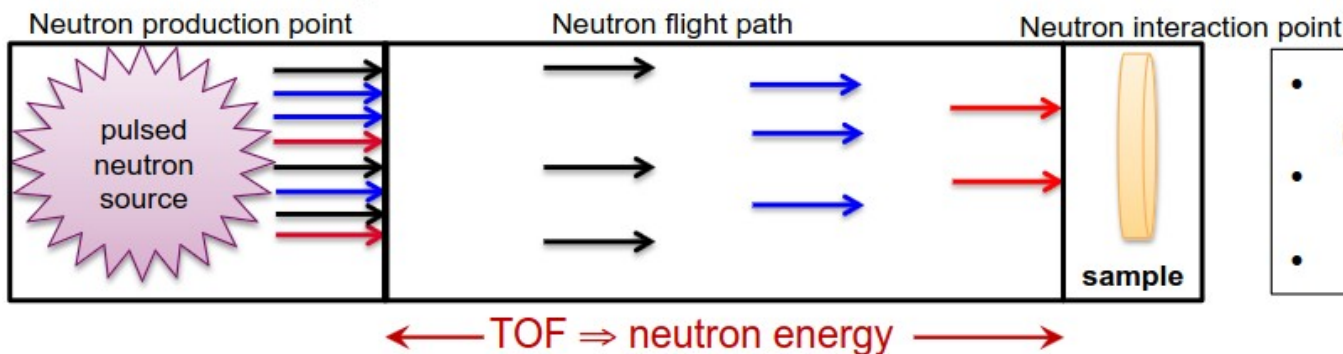
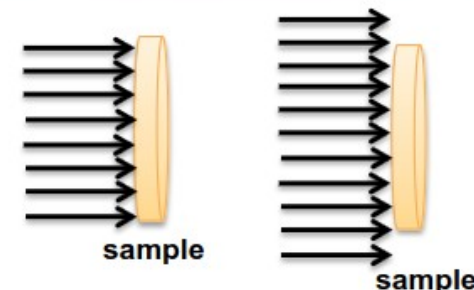
- **Neutron fluence/Beam interception factor**

Number/fraction of neutrons hitting the area covered by the sample.

- **Shape of the beam profile**

Beam optics misalignment => Beam fluence variations.

For **non-monoenergetic** neutron sources:

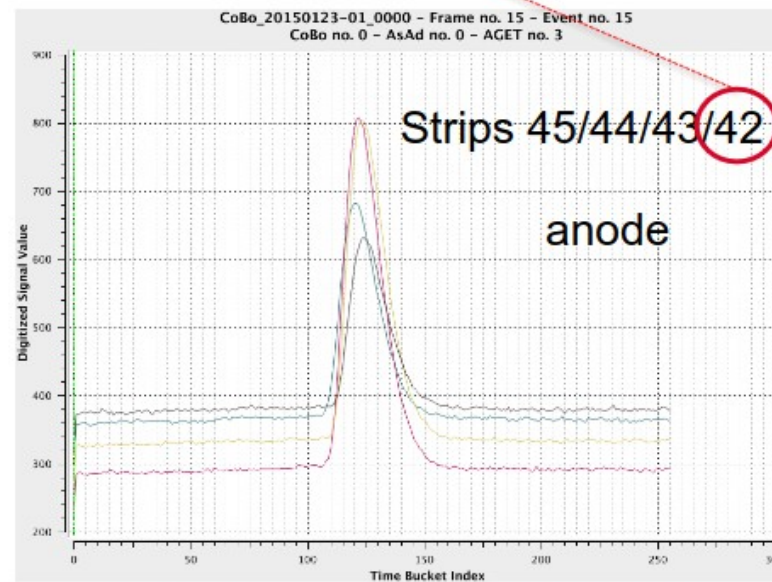
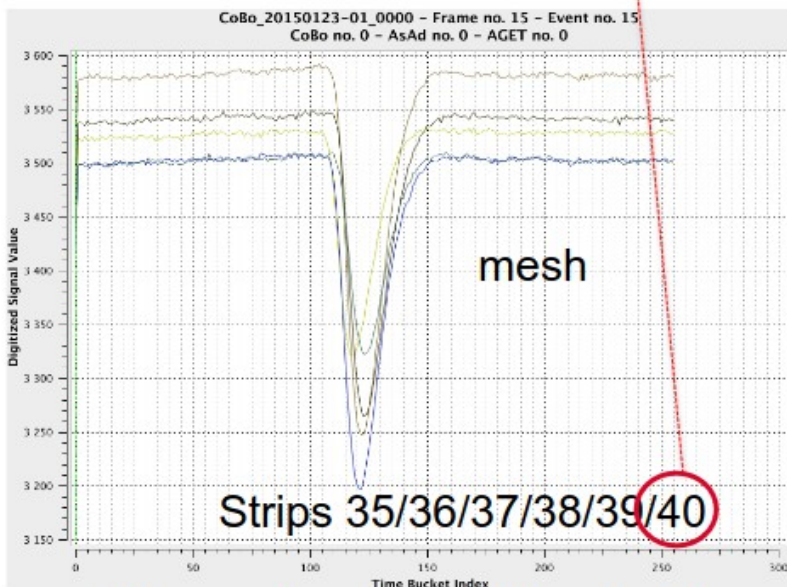
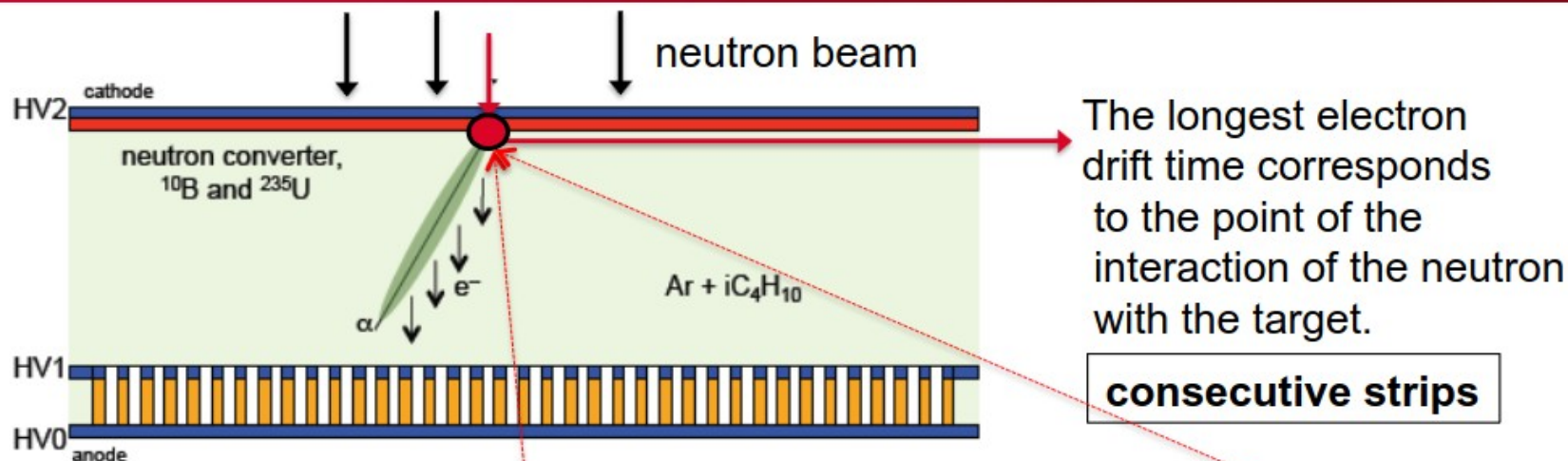


- n\_TOF facility (CERN) (thermal-GeV)
- GELINA (IRMM) (1meV-20MeV)
- NFS (GANIL)

=> **Dependence of profile on the neutron energy**

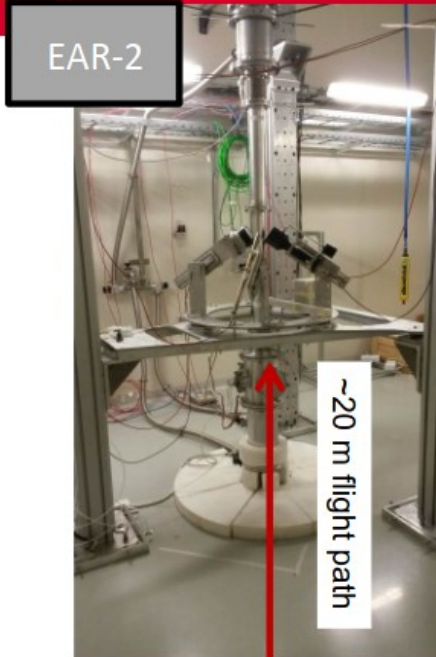
**Requirements:**

- Quasi-online neutron flux + beam profiler as well
- Minimal perturbation of the neutron beam / Minimal induced background
- Stay permanently in the beam



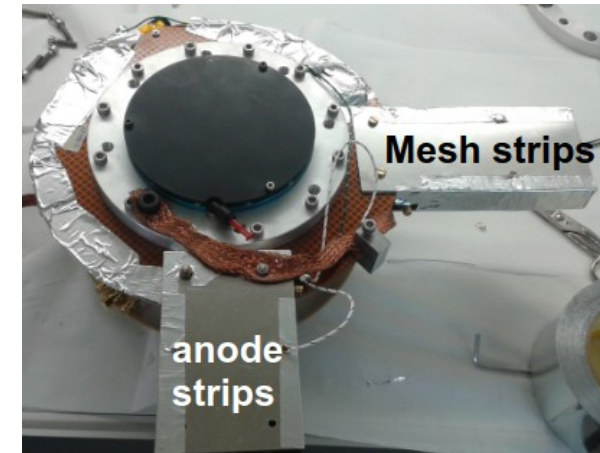
The neutron flux will be simultaneously extracted from the SUM SIGNAL.



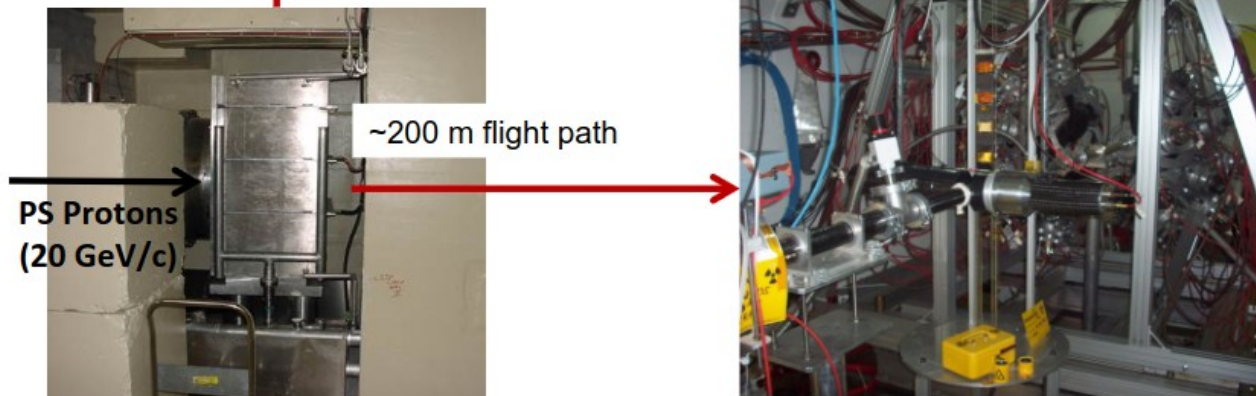


Neutron beam characteristics:

1. White neutron beam (0.025 eV-1 GeV).
2. Neutron energy defined by the Time-Of-Flight.
3. High instantaneous flux.
4. 7ns width proton pulse every > 1s
5. Excellent energy resolution



## MOUNTING THE DETECTOR IN EAR-2





- **Setup** of of 2x MMFE1s on 2x Resistive Micromegas chambers (Ar+7%CO<sub>2</sub> 400μm pitch, 5mm drift)
- Custom made **firmware** and **software** was developed allowing to **trigger** with scintillator system
  - Mode to control the CKBC externally
- **High data rate** ~20KHz/channel (VMM can reach 4MHz), arrived at the limit of Gbps UDP connection
- **Noise** levels of 300 e<sup>-</sup> ENC at gain 9mV/fC, 200ns

